

ACKNOWLEDGEMENTS

I want to thank all the people who had helped me on my research all through the past years. Particularly I would like to acknowledge some of them who did directly support me on this thesis.

First I would express my sincere gratitude to my advisor, Dr. Starzyk. It is him who first led me into the area of GPS. He offered insight directions to all my research topics. His professional advices always inspired me. I would like to thank Dr. van Graas for his guidance, patience and encouragements. His effort is very important to my research. Also Dr. Uijt de Haag must be specially thanked for being my committee member. Sincere thanks are for Dr. Matolak. From his courses about mobile communication, I did learn a lot that I had never been taught in other classes. The assistance provided by all the faculty members in the EECS School will never be forgotten.

This thesis would never be finished without the help of my friends, especially Jing Pang, Abdul Alaqeeli and Sanjeev Gunawardena. Their cooperation made it possible for me to complete my research quickly.

Finally, the support from my family gives me the opportunity to study here. All my energy to work on my research is from them.

TABLE OF CONTENTS

LIST OF TABLES	v
LIST OF ILLUSTRATIONS	vi
1. INTRODUCTION.....	1
2. GLOBAL POSITIONING SYSTEM.....	4
3. GPS SIGNAL PROCESSING	7
3.1 GPS Signal Structure.....	7
3.2 GPS Receiver Architecture	12
3.3 GPS signal processing- acquisition	14
3.3.1 Acquisition	14
3.3.2 Signal Power and Misdetection Probability	16
3.3.3 Demodulating Frequency	24
3.4 Tracking	25
3.4.1 Sequential Time Domain Tracking Loop.....	25
3.4.2 Correlation Based Tracking	28
3.5 Software Radio Introductions.....	30
3.6 Hardware Implementations	32
4 AVERAGING	33
4.1 Averaging Up Sampled Signal.....	33
4.2 Acquisition with Smaller FFT Blocks.....	36
4.3 Correlation using Block Processing	40
4.3.1 Zero Padding	40
4.3.2 Modified C/A Code	47
4.4 Correlation Based Tracking	48
5 WEAK SIGNAL ACQUISITION	53
5.1 Accumulation	54
5.1.1 Gain on Carrier to Noise Ratio.....	55
5.1.2 Effect on Signal Bandwidth and Interference	56
5.2 Time Domain Process	59
5.3 Frequency Domain Process	62
5.4 Block Addition for Weak Signal Acquisition	63
5.5 Performance Comparison.....	64
5.5.1 Carrier to Noise Ratio Gain.....	66
5.5.2 Computation Cost and Time	69
5.5.3 Interference Depression.....	70
5.6 Discussions of Block Addition.....	74

	iv
5.6.1 Accumulation Window Size and Navigation Data Bit.....	74
5.6.2 Combination of Block Addition and post correlation overlapping.....	74
5.6.3 Efficient Realization with Averaging.....	75
6. CONCLUSION AND FUTURE WORK.....	77
REFERENCES.....	79
ABSTRACT	82

LIST OF TABLES

Table 5. 1 C/N_0 Gain Comparison of Correlation Methods (on 10 ms signal).....	67
Table 5. 2 Computation Cost Comparison of Correlation Methods (on 10 ms signal)	71

LIST OF ILLUSTRATIONS

Fig. 2.1 A 2-D Positioning	5
Fig. 3. 1 Autocorrelation of M Sequences	10
Fig. 3. 2 Autocorrelation of C/A Code Sequences	11
Fig. 3. 3 Cross Correlation of M Sequences	13
Fig. 3. 4 Cross Correlation of C/A Code Sequences	13
Fig. 3. 5 GPS Receiver Block Diagram	13
Fig. 3. 6 2-D Search	16
Fig. 3. 7 PDF of Correlation Peak and Highest Noise	20
Fig. 3. 8 Misdetection Probability, Estimation and Simulation	22
Fig. 3. 9 Peak-to-peak Ratio V.S. C/N_0	23
Fig. 3. 10 Signal Energy Loss Due to Freq. Offset	25
Fig. 3. 11 Code Phase Tracking Loop Diagram	26
Fig. 3. 12 Discriminator Outputs	27
Fig. 3. 13 Triangular Fitting	29
Fig. 3. 14 Structure of Software Radio Receiver Digitized Front-end	31
Fig. 4. 1 The 5 Sequences of Averaged Steps	34
Fig. 4. 2 Worst Case of Code Phase	35
Fig. 4. 3 Discrete Correlation (part)	37
Fig. 4. 4 Correlation Result for Each of the 5 Sequences and C/A Code	37
Fig. 4. 5 Correlation Result for 2 of the 5 Sequences and C/A Code	37
Fig. 4. 6 Peak-to-peak Ratio Comparison of the Two Methods	39
Fig. 4. 7, 4. 8 Peak to the Second largest Ratio, Comparison of Two Methods	39
Fig. 4. 9 Correlation Zero Padding Sequences	41
Fig. 4. 10 Correlation of Zero Padding Sequences, $k = 1023$	44
Fig. 4. 11 Correlation of Non-zero Padding Sequences	44
Fig. 4. 12 Correlation of Zero Padding Sequences, at Selected Places	45
Fig. 4. 13 Correlation of Zero Padding Sequences, Based on Acquisition	49
Fig. 4. 14 Forming A Discrete Correlation	50
Fig. 4. 15 Fit-in Triangle	51
Fig. 4. 16 Accumulated Tracking Error	52
Fig. 5. 1 Correlation Using Sequential Accumulation Process	68
Fig. 5. 2 Correlation Using Post Correlation Overlapping	68
Fig. 5. 3 Correlation Using Block Processing	68
Fig. 5. 4 Post Correlation Overlapping, with Interference	73
Fig. 5. 5 Block Addition Correlation, with Interference	73
Fig. 5. 6 Block Addition Averaging Correlation	76

1. INTRODUCTION

Since the 1960s satellites have been applied in navigation. Satellite based personal navigation programs have already been launched and certain services are available now. There are two primary existing global navigation satellite systems (GNSSs), the United States's Global Positioning System (GPS) and the Russian Federation's Global Orbiting Navigation Satellite System (GLONASS) [Kayton, 1996]. More satellite navigation systems have been proposed or are in development, such as Europe's Galileo system. More GPS applications continue to develop, especially in the area of indoor positioning, which requires advanced signal processing to acquire and track weak signals. Due to its inherent limitations, hardware equipment alone cannot be held responsible for optimization of weak signal processing. Therefore, software radio technology has been introduced into GPS receiver design [Akos, 1997].

The last decade has witnessed a noticeable evolution in software radio technology. The complexity of signal processing algorithm realization makes this technology desired for many kinds of radio networks, including GPS [Bose, 1999], [Akos, 2001]. Complicated computations, for example, block processing, become feasible in receivers implemented with software radio technology.

Block processing is defined to implement required signal processing on blocks of received data. It could be widely used in signal processing in many communication and navigation systems. In GPS receivers, block processing is used to realize frequency

domain signal processing, which is capable of enhancing the performance and efficiency of receivers [Uijt de Haag, 1999], [Psiaki, 2001].

Using the block processing technique, GPS signal can be processed in frequency domain while traditional GPS receivers only do time domain processing. Software technology and frequency domain processing designs will change the basic structure of a GPS receiver. As discussed in this thesis, they would enrich GPS receivers' ability to determine the position of mobile users in the case that satellite signal is greatly attenuated. Several specific algorithms designed for weak signal applications have been proposed.

However, software radio design requires large hardware effort [Gunawardena, 2000]. Efficient solutions for hardware implementation are especially desired in software GPS receivers. Particularly, large amount of correlation computation needs to be realized. This thesis proposes the method "Averaging Correlation", which is proven to be a convenient realization of frequency domain correlation. Using this method, software radio technology can be applied for GPS receivers with general-purpose processing blocks. Algorithms for weak signal processing can also be performed based on "Averaging Correlation". These algorithms are introduced, evaluated and compared with their hardware implementation also considered and "Block Addition" has been found with better performance, as shown in this thesis.

The thesis will be presented in 6 parts, beginning with this introduction. The second chapter is Global Positioning System introduction, followed by GPS signal processing, in Chapter 3. Chapter 4 proposes a new method called averaging correlation

and discusses its realization. After that weak signal acquisition methods are demonstrated and compared in Chapter 5. One acquisition method will be emphasized and it can be realized with averaging correlation. Conclusion and future work are given in Chapter 6.

2. GLOBAL POSITIONING SYSTEM

The Global Positioning System (GPS) is a satellite-based navigation system consisting of a network of at least 24 positioning satellites that are in 6 orbits eleven thousand miles from Earth. Although the system was originally designed purely for military purposes, eventually two levels of positioning services are provided, Precise Positioning Services (PPS) and Standard Positioning Services (SPS). Only SPS is accessible to civil users until now. Besides positioning GPS also provides velocity measurements, as a complete navigation system and works as the major precise timing provider in the U. S. A.

Doing positioning, users measure the distances to several visible satellites and then apply geometric techniques to determine their three-dimensional (3-D) position at a certain level of precision and ambiguity. A 2-D positioning can be illustrated in the following figure, as an example of the geometric technique shown in Fig. 2.1. Two points come out as possible solutions based on the measurements of distances to the two centers. In reality, one point will be found far away from Earth and the other is taken as the result. Consequentially 3-D positioning needs at least 3 centers. The precision of distance measurements directly determines the positioning precision.

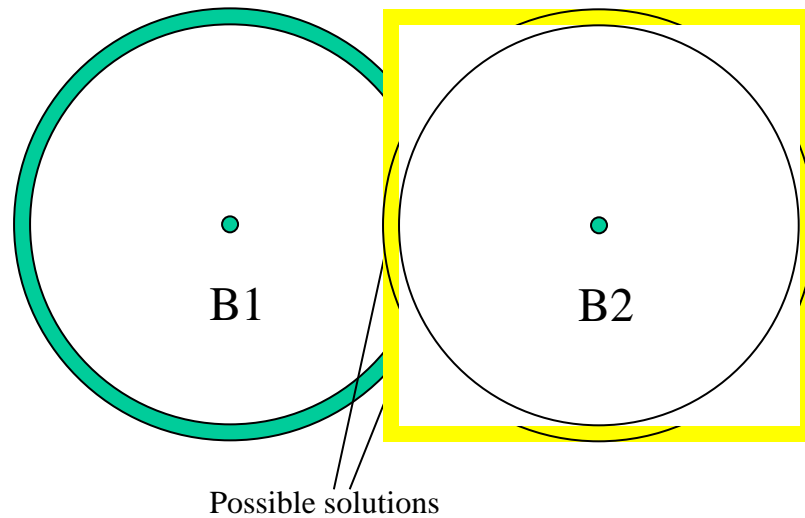


Fig. 2. 1 A 2-D Positioning

Distance can be calculated based on the signal propagation delay from satellites to receivers as in the following equation.

$$PR = c(ToR - ToT) \quad (2.1)$$

Where c is the speed of light, PR is measured Pseudo Range, ToR and ToT stand for receiving and transmitting time respectively.

Satellites record the leaving time of a particular piece of signal and add this information onto a succeeding signal. Receivers measure the arriving time of the signal and read the information to obtain the propagation time and therefore figure out the range.

The measurement is named as GPS Pseudo Range instead of the true range, because receiver clocks are not perfectly synchronized with satellite transmitters' clocks.

It is normally hard for receiver clocks to achieve the same precision as satellite clocks'.

The clock offset between receivers and satellites is quite hard to predict and its effect on range measurements should be determined together with the 3-D position coordinates.

The fourth unknown variable, clock offset can be represented by b .

$$R = PR + \Delta = c(ToR - ToT + b) \quad (2.2)$$

$$PR = |SV_{x,y,z} - RX_{x,y,z}| - c \cdot b \quad (2.3)$$

Where R is the true range and b is unknown receiver clock offset. $SV_{x,y,z}$ and $RX_{x,y,z}$ represent the three dimensional coordinates of satellites and receivers. Therefore, 4 parameters, including three position coordinates and the clock offset of receivers, need to be solved for the pseudo range measurements. As the result, at least 4 satellites are required to meet the basic requirements for positioning. It should be noticed that if a good geometry is required to improve precision, more than 4 satellites may be needed.

3. GPS SIGNAL PROCESSING

3.1 GPS Signal Structure

GPS employs binary phase shift keying (BPSK) modulated direct sequence spread spectrum (DSSS) signal. The GPS signal not only carries the information broadcast by the satellites but also indicates the propagation time and pseudo range measurements, as mentioned in Chapter 2. Currently two carrier frequencies L1 and L2 are used. There are two types of pseudo random noise (PRN) sequences, C/A code and P-code, modulated on L1 carrier, with one P-code only modulated on L2. Using asynchronous code division multiple access (a-CDMA) technologies, as most satellite CDMA systems do, navigation data is despread based on top of both C/A and P-codes. The signal at L1 can be expressed as:

$$s_j(t) = A_j C A_j(t) P_j(t) X_j(t) D_j(t) \cos((\omega + \Delta\omega_j(t))t + \phi) \quad (3.1)$$

Where:

$s_j(t)$: signal transmitted from jth satellite

$A_j(t)$: signal amplitude

$C A_j(t)$: C/A code assigned to this satellite, chipping rate 1.023 Mcps

$P_j(t)$: P code assigned to this satellite , chipping rate 10.23 Mcps

$X_j(t)$: X code, optional encryption of P code

$D_j(t)$: navigation data broadcasted by jth satellite, data rate 50 bps

ω : L1 carrier frequency, $2\pi \times 1575.42 \text{ MHz}$

$\Delta\omega_j(t)$: carrier frequency shift

ϕ : original signal phase

The P-code is encrypted with X-code for military purposes. The chipping rate of the P-code is 10.23 mega chips per second (Mcps) and the whole sequence repeats every 267 days. However each satellite only uses a portion of P-code with the length of 7 days. The C/A code has a period of 1023 chips with the chipping rate of 1.023 Mcps, therefore, the C/A code repeats every millisecond. Each satellite is assigned a unique C/A code. In addition to the original purpose of assisting the P-code positioning, C/A code is accessible to all civilian users as a positioning code while P-code is for authorized users only. This thesis is mainly concerned with C/A code.

The auto correlation and cross-correlation properties of these PRN codes form the fundament of pseudo-range measurements and navigation data modulation. C/A code correlation functions will be the main focus of the following sections.

For a binary code, auto correlation can be defined as:

$$\Phi_{rr}[m] = \frac{1}{L} \sum_{n=0}^{L-1} r[n]r[n-m] \quad (3.2)$$

Where r is the random binary code with length L .

Ideally,

$$E(\Phi_{rr}[m]) = \Phi_{rr}[m] \cdot \delta[m] = \Phi_{rr}[0] \cdot \delta[m] \quad (3.3)$$

Where $\delta[m] = 1$ when $m = 0$, otherwise it is 0.

The cross correlation between sequences r and r' is:

$$\Phi_{rr'}[m] = \frac{1}{L} \sum_{n=0}^{L-1} r[n]r'[n-m] \quad (3.4)$$

Where r' is assumed to be another random sequence. The cross correlation is expected to be zero:

$$E(\Phi_{rr'}[m]) = 0 \quad (3.5)$$

The C/A code is not a truly random code. It is generated as the combination of two M-sequences using modulo-2 addition. This kind of combined code is known as a “Gold Code” [Gold, 1967], [Kaplan, 1996]. As a basic feature of M-sequences, the auto correlation function appears as:

$$\Phi_{MM}[m] = \frac{1}{L} \sum_{n=0}^{L-1} M[n]M[\text{mod}(n-m, L)] = \begin{cases} L & m = 0 \\ -1 & m \neq 0 \end{cases} \quad (3.6)$$

Where M is a M-sequence of length L. $m < L$, $L = 2^{n-1}$ and n must be an positive integer. Notice that M sequence is continuous and periodic, so the correlation could be defined as circular correlation based on a single period of signal, as in Eq. 3.6. The correlation functions of all the periodic signals, as C/A code, can be realized in form of circular correlation.

$\Phi_{MM}[m]$ is plotted when $L = 1023$:

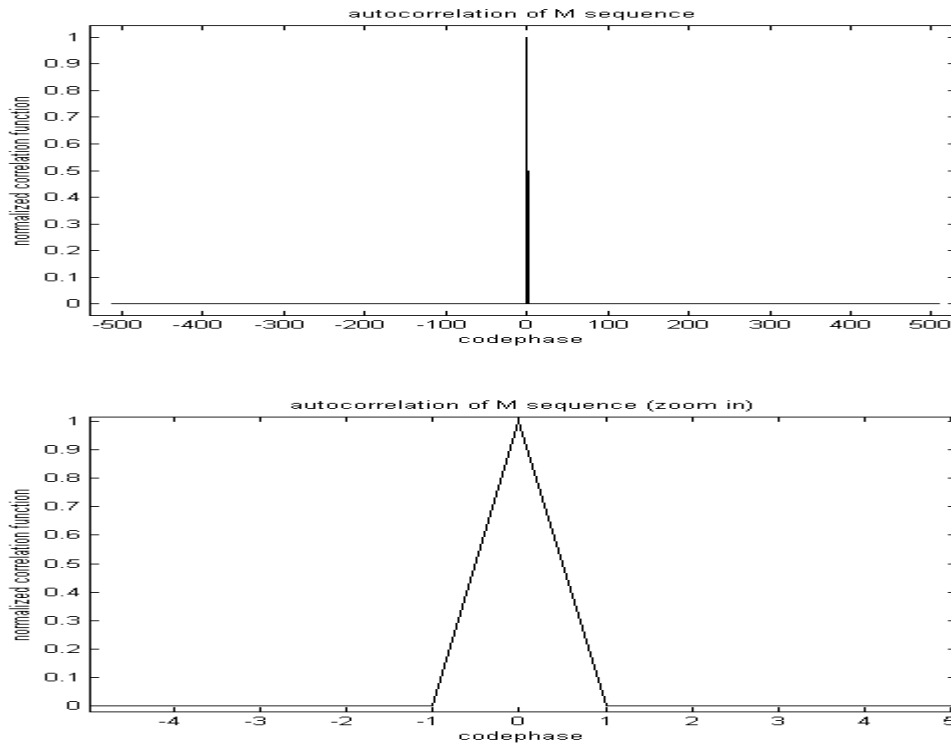


Fig. 3. 1 Autocorrelation of M Sequences

As can be seen from Fig. 3.1, autocorrelation of M sequences has only one main correlation peak standing above a flat floor. CDMA despreading detection can be reliable because there is no “side lobes”, where side lobes are the small peaks (local maximum) of the correlation function. Side lobes can be observed in the Gold code auto correlation functions. For instance, C/A code is a Gold code with $L = 1023$, and its auto correlation function Φ_{CACA} is shown in Fig. 3.2.

In practice C/A code autocorrelation is expressed in a slightly different way:

$$\Phi_{CACA}[m] = \frac{1}{L} \sum_{n=0}^{L-1} CA[n]CA'[\text{mod}(n-m, L)] \quad (3.7)$$

Where $CA'[n] = \begin{cases} CA[n-k], n \geq k \\ CA[L+n-k], n < k \end{cases}$, is CA shifted to the right by k chips.

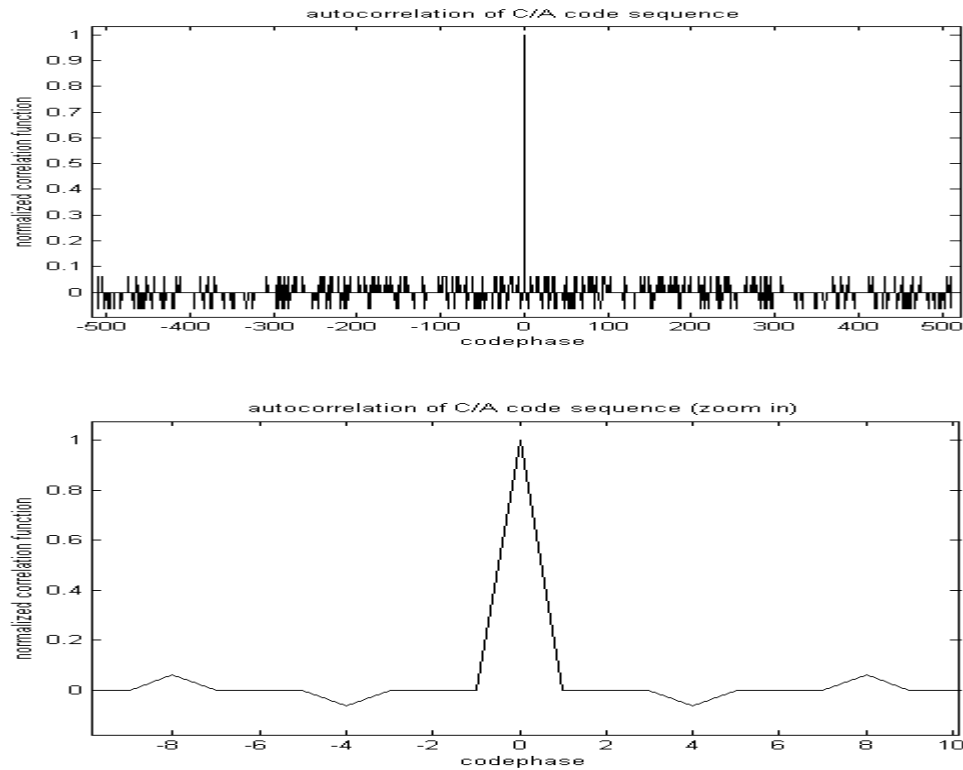


Fig. 3. 2 Autocorrelation of C/A Code Sequences

Obviously $\Phi_{CACA}[k]=1$. Here k is named the code phase, which indicates the relative shift between CA and CA'. In GPS receivers, the correlation function of received signal and receiver generated C/A code at code phase k , $\Phi[k]$, represents signal energy. In addition, the precise code phase, which is a time shift beyond chip level in reality, provides propagation time measurements in signal tracking. Knowing this propagation time, the range measurements can be obtained from Eq. 2.1.

It can be seen from Fig. 3.2 that except for the highest correlation peak, there are some side lobes and they may increase misdetection probability in asynchronous CDMA

despreading. However, in spite of side lobes in its autocorrelation, Gold Code is still used in practice instead of M sequence, because it has bounded and stable cross correlation features [Kaplan, 1996]. At the same time M sequences' cross correlation could be as large as auto correlations, as shown in Fig. 3.3 and 3.4. Since all the GPS satellites use different positioning code sequences, cross correlation of different C/A code sequences indicate the self-interference of GPS. Poor cross correlation of M sequences makes it unacceptable for GPS; while Gold code provides limited inter channel interference for a-CDMA (asynchronous CDMA) system. C/A code is thus designed as a Gold code with length of 1023 chips. A large processing gain of spreading code is not common in communication systems, however it is needed for GPS satellites to provide smaller bit error probability at the price of slow navigation data rate.

Correlation functions of the GPS PRN codes form the base of all the subsequential processes in a GPS receiver, including 2-D search, demodulation, acquisition and tracking.

3.2 GPS Receiver Architecture

A simplified GPS receiver architecture is shown in Fig. 3.5.

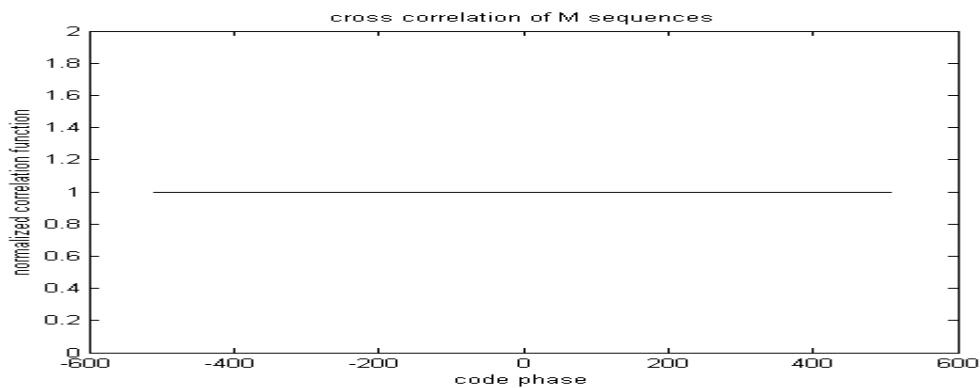


Fig. 3. 3 Cross Correlation of M Sequences

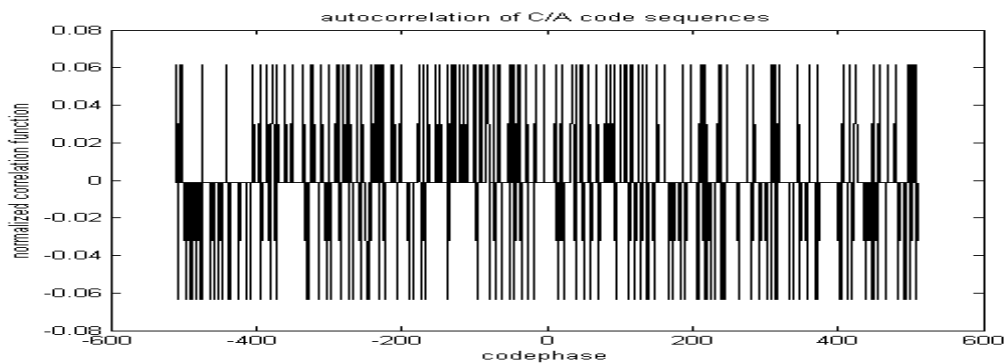


Fig. 3. 4 Cross Correlation of C/A Code Sequences

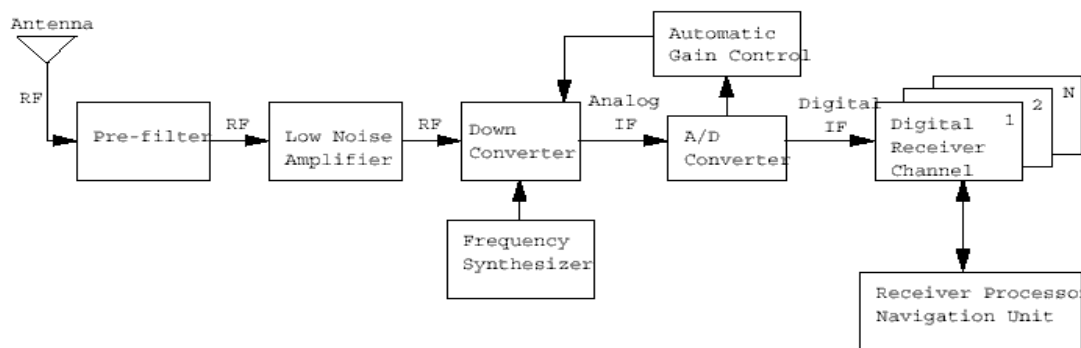


Fig. 3. 5 GPS Receiver Block Diagram [Hegarty, 1999]

The GPS signal, as defined above, is received from an antenna and sent through all the stages of the front end. It is amplified and down converted from carrier frequency (f_c) to a lower intermediate frequency (IF). The output signal of the front-end is sampled at the A/D converter. Since the carrier frequency has already been down converted to intermediate frequency (IF), the sampling rate has to be at least twice as large as IF in order to satisfy Nyquist's Law. Typically non-coherent demodulation is applied in receivers to deal with the digitized IF. As mentioned before, asynchronous code despreading is applied. Signal needs to be acquired first and then tracked. Based on acquisition and tracking, pseudo range measurements and navigation data can be obtained.

3.3 GPS Signal Processing- Acquisition

3.3.1 Acquisition

Obviously signal cannot be demodulated when the three items are unknown to a receiver: 1) the received code, which is unique to each satellite, 2) code phase, which indicates the signal energy at correlation functions, and 3) carrier frequency (IF) offset, which is mostly due to Doppler effects and limited precision of receiver clocks. The procedure that establishes these three parameters is called acquisition. Once these three parameters can be determined, the signal is acquired and C/A code acquisition is a necessary initial stage to all the other signal processing.

Searching for three parameters at the same time may not be necessary since prior knowledge of all the satellites orbits can guide receivers only to try acquiring signal from a few visible satellites. Although carrier frequency and IF is pre-designed for GPS satellites and receivers, relative motion between receiver antennas and satellites will bring in Doppler frequency components as the uncertainty of carrier frequency and IF. Receiver clock frequency offset also contributes to this uncertainty. Thus the demodulating frequency needs to be detected within the uncertainty range of the IF value. The difference between the demodulating IF and the real IF causes loss of signal energy, as will be further explained in more details. In practice, the detection of IF is actually realized as a search with certain frequency steps in order to have the largest demodulated signal energy. Note that signal energy can be represented with the correlation function of received C/A code sequence and local code sequence. As mentioned before, the correlation function has a peak value when there is no relative shift between the two sequences.

The problem is that the phase of the C/A code inside the received signal is unknown to receivers before acquisition. Thus at each IF search step the signal energy detection is also regarded as search of code phase. Therefore the acquisition of C/A code could be considered as a 2-D search, meaning search for IF and code phase.

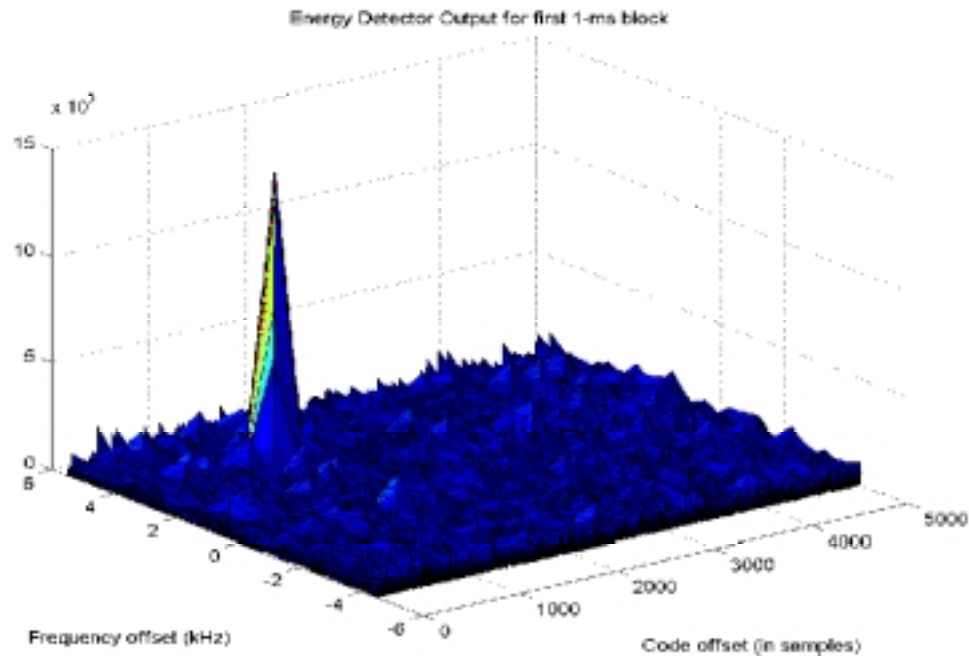


Fig. 3. 6 2-D Search

3.3.2 Signal Power and Misdetection Probability

If the signal energy, or to say correlation peak does obviously stand above the noise level, the correlation peak can easily be detected. This leads to acquisition failure or misdetection.

With noise and correlation side lobes, the cross correlation function of received C/A code and local code can be observed with more than 1 peak. Hopefully the highest one of all the apparent peaks represents the true correlation peak and indicates the code phase while others are all caused by noise and/or side lobes. In practice the ratio of the highest peak to the next largest peak, known as peak-to-peak ratio, is used to examine

how strong the signal is against noise. Statistically, this peak-to-peak ratio increases with stronger signal and larger peak-to-peak ratio assures smaller misdetection probability. Note that this ratio is not accurate in case of strong noise component. Only when averaged peak-to-peak ratio exceeds a certain level, for instance, 2, acquisition could be credible enough. Numerical analysis is needed to precisely determine the misdetection probability.

The relationship between the signal power and the noise level in GPS signal can be described with carrier-to-noise ratio (C/N_0). For example, C/A code at L1 frequency has the effective power level of 478.63W. Considering free space loss and assuming the distance between satellites and receivers is 20,000km. The received signal power level can be estimated as $P = -157.6$ dBw [Braasch, 1999], for example. Noise power is related to effective noise temperature T and front end bandwidth B : $N = kTB = -138.5$ dBw, where Boltzmann's constant $k = 1.3806 \times 10^{-23} J \cdot K^{-1}$, the effective noise temperature T is assumed to be 513K, and bandwidth $B = 2$ MHz. Signal to noise ratio can be defined as:

$$S/N_0 = \frac{P}{N} = P - N(\text{dB}) \quad (3.8)$$

$$\text{SNR} = -157.6 - (-138.5) = -19.1(\text{dB}).$$

However, C/A code correlation despreads the signal and the bandwidth is reduced to bandwidth of navigation data, $B_d = 50$ Hz. Although neither the signal power nor the noise level is changed, S/N_0 becomes different due to the despreading. Alternately, carrier to noise density ratio is defined:

$$C/N_0 = S/N_0 \cdot B \quad (3.9)$$

Which is described as the relative noise level. For the example above,
 $C/N_0 = S/N_0 + B(\text{dB}) = 43.9\text{dB} - \text{Hz}$.

Normally C/N_0 ranges from 35 to 55 dB-Hz. It can be observed that for GPS signal with C/N_0 less than 43 dB-Hz, it is hard to do C/A code acquisition using 1 ms signal, simply because the probability of noise standing higher than the correlation peak is too high.

Probability of misdetection can be estimated for the base band signal. Using unified signal power, the variance of noise can be expressed as $\sigma^2 = \text{var}(N) = \frac{B}{C/N_0}$.

Using bandwidth of 2MHz, for the normal configuration of GPS receivers and using the channel model as Additive White Gaussian Noise corrupted channel the noise variance can be calculated according to various C/N_0 .

For C/A code acquisition, certain assumptions are made to simplify the analysis. The signal sampling rate is set the same as the chipping rate of 1.023 Mcps (Mega chips per second). Note that the noise on each sample of received signal is independent. When the received signal is correlated with the local C/A code, the noise is also correlated with the C/A code. Since the C/A code is pseudo randomly generated, the correlated noise samples are assumed to be independent with each other in this analysis. Thus the variance of correlated noise is $\sigma_n^2 = L\sigma^2 = \text{var}(N)$, $L = 1023$ for the sampling rate of 1.023 Msps (Mega samples per second). The auto correlation of C/A code is assumed to be no side lobes, which is only valid to the M-sequence auto correlation. In this simplified

correlation function there will be one sample representing the correlation peak. In the noise free case, this peak sample should be L and all the other samples should be -1 .

Therefore all the samples in correlation function are assumed to be Gaussian distributed. The peak sample has the mean value L and standard deviation σ_n . All the other samples are noise samples, with mean value -1 and standard deviation σ_n .

The misdetection probability can be estimated as a function of σ_n :

$$P_m = \int_{-\infty}^{+\infty} P_1(x) \frac{dP_2(x)}{dx} dx \quad (3.10)$$

Where P_1 is defined as the probability for the correlation peak smaller than x :

$P_1 = P(\text{peak} < x)$. P_1 is the cumulative distribution function (CDF) of the peak sample.

P_2 is defined as the CDF of the largest noisy sample in the correlation function, except for the peak:

$$P_2 = [P_3(\text{noise} < x)]^{L-1}$$

Where $L = 1023$, according to the sampling rate, P_3 stands for the CDF of a single noise sample [Stuber, 2001]. As assumed, it is Gaussian distributed, with mean value -1 and standard deviation σ_n .

Probability density function (PDF) of the correlation peak sample and highest noise sample can be observed in Fig 3.7.

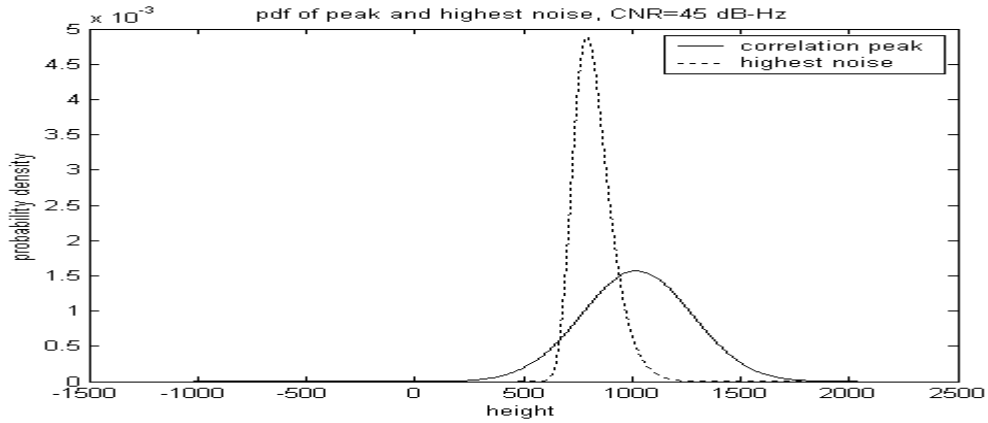


Fig. 3. 7 PDF of Correlation Peak and Highest Noise

Misdetection happens when largest noise exceeds the peak and Eq. 3.10 has been obtained.

The misdetection probability can be estimated:

$$P_m = (L-1) \int_{-\infty}^{+\infty} P_1(x) P_3^{L-2}(x) \frac{dP_3}{dx} dx \quad (3.11)$$

Where:

$$P_1(x) = \int_{-\infty}^x \frac{1}{\sqrt{2\pi}\sigma_n} e^{-\frac{(y-L)^2}{2\sigma_n^2}} dy$$

$$P_3(x) = \int_{-\infty}^x \frac{1}{\sqrt{2\pi}\sigma_n} e^{-\frac{(y+1)^2}{2\sigma_n^2}} dy$$

$$\frac{dP_3}{dx} = \frac{1}{\sqrt{2\pi}\sigma_n} e^{-\frac{(x+1)^2}{2\sigma_n^2}}$$

Besides the theoretical estimation of Eq. 3.11, the acquisition based on the same assumption has also been simulated in software with $L=1023$. Also the correlation

function is assumed to have no side lobes. Simulated results appear very close to the estimation of misdetection probability using Eq. 3.11, as can be observed in Fig. 3.8.

Simulation and estimation can be further expanded to the up sampled signal, which is close to the real cases. Especially for the signal up sampled at 5 Msps, where $L = 5000$, the misdetection probability can be estimated. For the correlation function of the up-sampled signal, noise is no longer independent. Thus $\sigma_n^2 = L\sigma^2$ is no longer correct, as used in Eq 3.10 and 3.11. Furthermore, up-sampled signal has 4 to 5 samples corresponding to a single chip, for instance, the code phase chip. Detection of any one of them could be considered as a successful acquisition. In Eq. 3.11 only one sample will be regarded as the true code phase while the others are regarded as false detection. This yields misdetection probability derivation different from the one described in Eq. 3.11.

However, experiments show that estimation using Eq. 3.11 is still a close approximation of the misdetection probability of the signal up sampled at 5 Msps, as shown in Fig. 3.8.

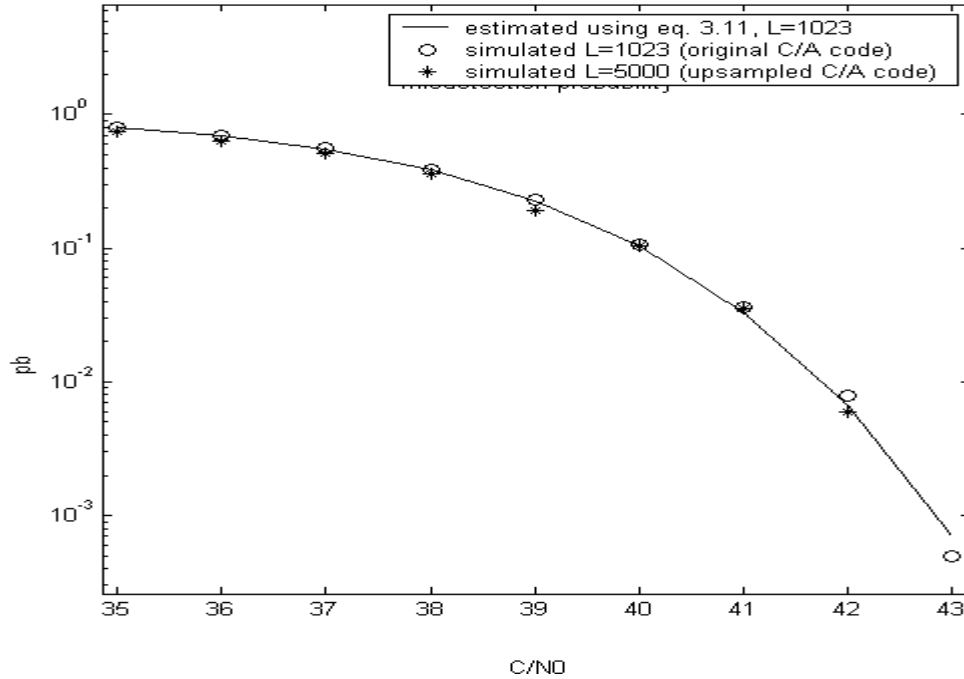


Fig. 3. 8 Misdetection Probability, Estimation and Simulation

As mentioned at the beginning of this section, a direct metric of the signal strength is the peak-to-peak ratio. The information of carrier to noise ratio could be roughly obtained from averaged peak-to-peak ratio.

Again the signal power is unified so that peak-to-peak ratio can be estimated as a function of σ_n . Assume the sampling rate of 1.023 Msps. Expected value of the correlation peak: $E(\text{peak}) = L = 1023$.

Expected highest noise sample level, excluding side lobe:

$$E(n\text{peak}) = \int_{-\infty}^{+\infty} xp(x)dx \quad (3.12)$$

Where $p(x)$ is the probability density function of highest noisy sample, as shown in Fig. 3.7:

$$p(x) = \frac{dP_2(x)}{dx} = (L-1)P_3^{L-2}(x) \frac{1}{\sqrt{2\pi}\sigma_n} e^{-\frac{(x+1)^2}{2\sigma_n^2}}$$

and $P_2(x) = P_3^{L-1}(x)$ represents the CDF for the highest noisy sample, as previously defined. Using the expected value of the correlation peak and the highest noisy sample level, the peak-to-peak ratio (acquisition margin) can be estimated based on the noise variance

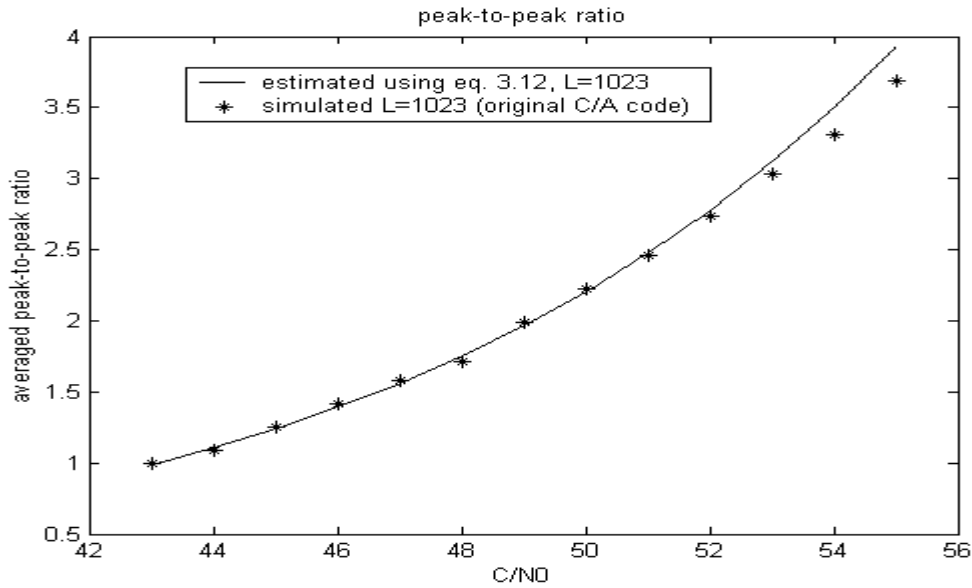


Fig. 3. 9 Peak-to-peak Ratio V.S. C/N₀

Fig. 3.9 shows the relationship between expected peak-to-peak ratio and C/N₀. The simulated results are based on C/A code correlation functions. Due to the effects of

side lobes, the simulated peak-to-peak ratio appears different with estimated. The difference may be as large as 6% and is most significant for high C/N_0 cases.

Therefore, direct observations on the received signal correlation function will allow the estimation of misdetection probability in relatively strong signal cases, i.e. 43 dB-Hz or above. Once the peak-to-peak ratio can be counted, the rough C/N_0 value will be known based on Fig. 3.9. Using Fig. 3.8, misdetection probability can be easily found. Thus the relationship between C/N_0 , acquisition margin and misdetection probability has been analytically established.

Previous estimations and simulations are all performed in the base-band without taking the effect of IF demodulation into account. As mentioned above, the signal energy or the correlation peak suffers great loss due to demodulation frequency inaccuracy. This also changes the misdetection probability.

3.3.3 Demodulating Frequency

For CDMA despreading, correlation function values are the function of demodulation frequency deviation and incoming signal bandwidth, no matter for desired signal or interferences, as shown in Fig. 3.10 [Uijt de Haag, 1999], [Feng, 1999].

$$S(\omega, B_s) = \left(\frac{\sin(0.5\Delta\omega / B_s)}{0.5\Delta\omega / B_s} \right)^2 \quad (3.13)$$

Where S is the detected signal energy (normalized), $\Delta\omega$ is the demodulation frequency deviation and B_s stands for incoming signal bandwidth. For example N millisecond continuous signal has the bandwidth $B_s = \frac{1}{N} \text{kHz}$.

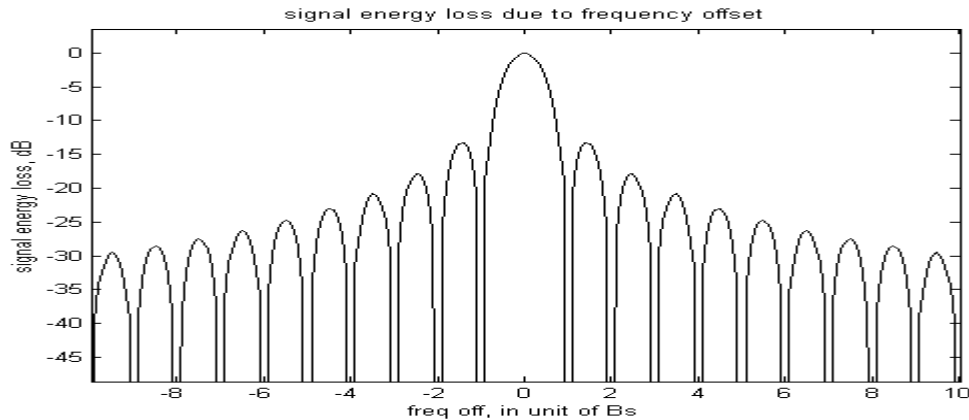


Fig. 3. 10 Signal Energy Loss Due to Freq. Offset

This feature shows that demodulating frequency should be carefully selected or searched in order to avoid the large loss of signal energy. As explained section 3.1, this signal energy is represented by the correlation peak. Another potential usage is that this feature depresses the self-interference of GPS signal. It will be further exploited in weak signal acquisition discussed in Section 5.1.2.

3.4 Tracking

3.4.1 Sequential Time Domain Tracking Loop

After the signal is acquired, the receivers need to start a the tracking loop to ensure that modulation frequency and code phase still match the incoming signal, in another word, keep tracking the precise code phase. Fig 3.11 demonstrates a block diagram of this loop in a typical sequential GPS receiver:

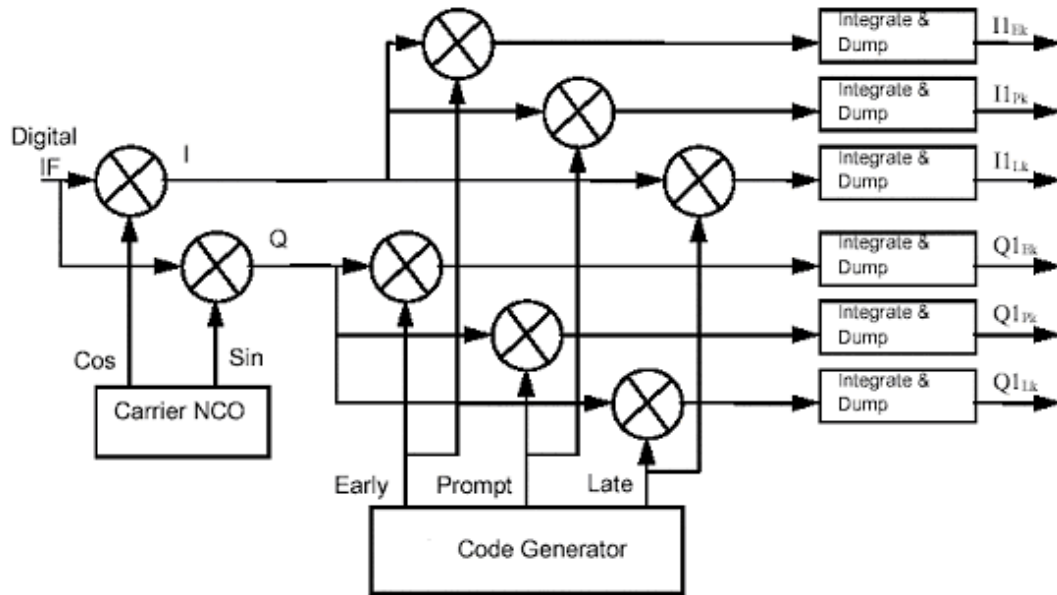


Fig. 3. 11 Code Phase Tracking Loop Diagram [Hegarty, 1999]

Code phase indicates propagation time changing during certain period and therefore delta pseudo range can be obtained. Accumulation of delta pseudo range will obviously provide pseudo range measurement.

As can be seen in this tracking loop, code phase detectors, named as discriminators contain three correlators, a prompt one, an early one and a late one. The prompt one calculates the correlation of received C/A code and a C/A code sequence assumed to be in phase with the received one. Early one does correlation of received code and a sequence with the phase leading by a small time, for instance, half chip length,

while the later one uses the sequence lagging by the same time. Their functions can be combined as discriminators.

Discriminator output can be formed as: [Braasch, 1999]

Using coherent demodulation:

$$D = (I_E - I_L) \text{sign}(I_P) \quad (3.14)$$

Or using non-coherent demodulation:

$$D = (I_E^2 + Q_E^2) - (I_L^2 + Q_L^2) \quad (3.15)$$

Or

$$D = (I_E - I_L) I_P + (Q_E - Q_L) Q_P \quad (3.16)$$

Where I and Q indicate in phase and quadratural energy parts of R respectively and subscripts E, L and P mean early late and prompt, respectively. They can be observed in Fig. 3.12.

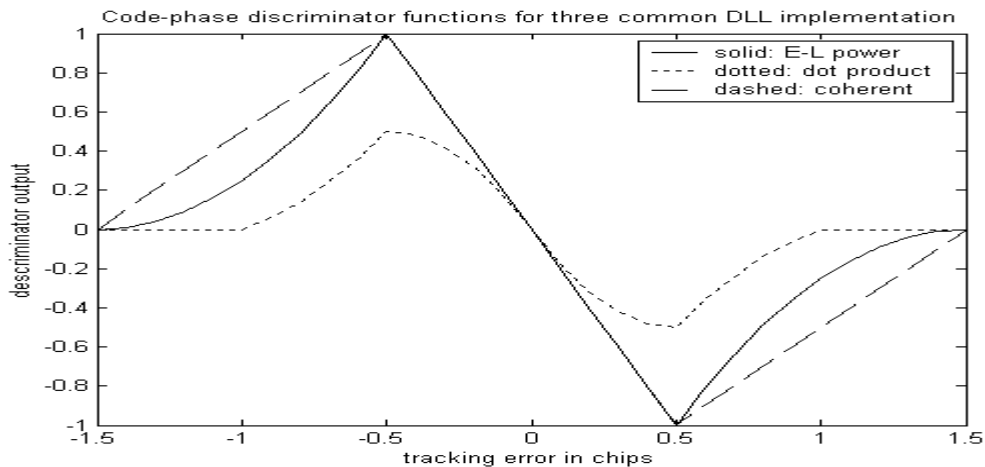


Fig. 3. 12 Discriminator Outputs [Braasch, 1999]

If the discriminator output is detected to be zero, the prompt sequence has the exact same code phase as the received one and the signal is tracked.

Notice that all the correlators are implemented in time domain and they are doing aperiodic sequential correlation. Since C/A code is actually repeating each millisecond and the noise on the received signal is totally random, this correlation can also be accomplished in form of a circular correlation in frequency domain with the help of software technologies, as introduced in section 3.5. Frequency domain processing not only changes the realization of correlators but also triggers a new architecture of GPS receiver. Acquisition and tracking may become more efficient in this new structure. For instance, tracking can be based on correlation functions instead of discriminator outputs.

3.4.2 Correlation Based Tracking

Knowing this correlation function, the code phase can be tracked without using discriminators. It is hard to directly point out the code phase from correlation function of digitized sequences, since the correlation function is also discrete. And the true code phase may be located somewhere between two samples. On the other hand, if the code phase can only be located at the sample level, tracking precision is really poor. For instance, maximal tracking error can be as large as half of sampling distance. For a SPS receiver with sampling rate of 5 Msps, the maximal error is 0.1 microseconds, corresponding to 30 meters in pseudo range measurement, which is not acceptable for tracking. The correlation function of the received signal and the local code has an

asymmetric peak with a curved top, as observed in Fig. 3.12, due to noise, multi path, signal distortion and all the other possible effects. Certain techniques can be applied to precisely locate the code phase based on this discrete correlation function.

Recall that in time domain we need to process three correlations to form the discriminator to monitor the code phase. They are based on the assumption that correlation peaks are symmetrical triangles. A similar technique can be applied to obtain the code phase from correlation function itself without using discriminators.

The correlation peak is known to be a triangle with the width of 2 chips. Although its actual shape is due to signal strength plus noise, the information of width and shape is exploited to find out a best place to fit in a triangle into the discrete correlation function.

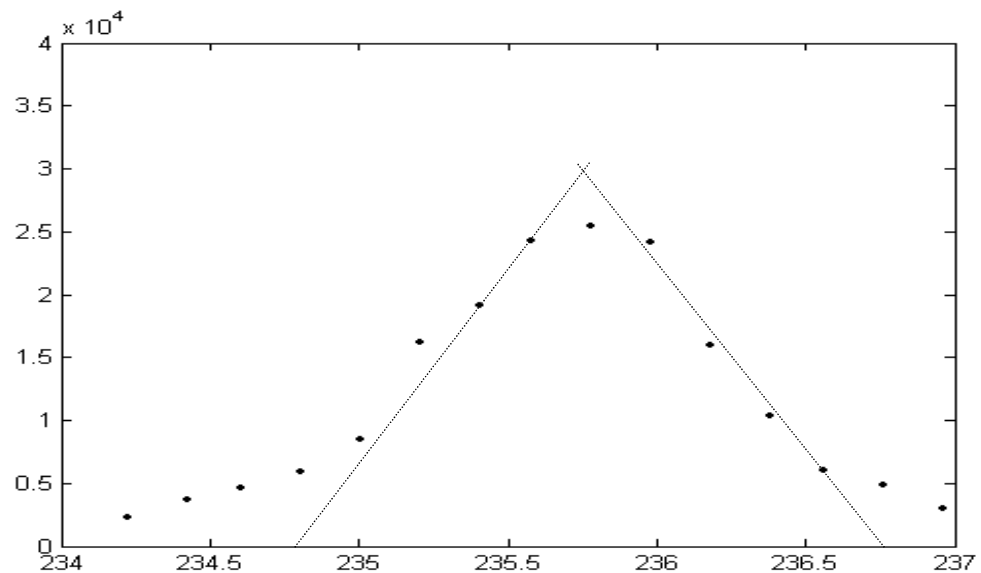


Fig. 3. 13 Triangular Fitting

Based on this fit-in triangle, as shown in Fig. 3.13, the code phase is determined as the top projection onto the time shift axis.

Since the signal bandwidth is limited (for example, 2 MHz) the binary chips cannot be represented as ideal square waveforms. Instead, they are distorted and therefore their correlation peak top appears to be a curve instead of a sharp angle. The triangular shape fitting can also be changed to a polynomial curve fitting to figure out the exact code phase. However, the method only focuses on the top shape without using the information of peak width, which is very important. It is not as accurate as it is assumed to be since the curve is not symmetrical. Neither is it as efficient as triangular shape fitting, especially in hardware implementation.

As a result, triangular shape fitting is used in the correlation function based tracking. An application will be discussed in section 4.4.

3.5 Software Radio Introductions

Obviously correlation function is concerned everywhere in acquisition and tracking. The way to compute correlation is actually a core part of GPS C/A code receiver design.

Similar to Eq. 3.7, correlation of the received signal S , which is a C/A sequence with noise and the corresponding receiver generated C/A code is:

$$\Phi_{SCA}[m] = \sum_{n=0}^{L-1} S[n]CA[\text{mod}(n-m, L)]$$

S and CA have the same length.

Define circular correlation as:

$$\Phi_{SCA}[m] = S[n] \otimes CA[n] \quad (3.17)$$

Since C/A code is periodic, its correlation can be replaced by circular correlation, in presence of random noise. It has been proven that circular correlation can be efficiently accomplished in frequency domain processing using Fast Fourier Transform (FFT).

$$S[n] \otimes CA[n] = iFFT[FFT(S[n]) \cdot FFT^*(CA[n])] \quad (3.18)$$

Where * means taking conjugate of.

Obviously this change needs implementation of FFT on the discrete signal, which has to be realized with software radio technologies.

The fundamental idea of software radio design can be simply described as follows [Akos, 1997]. An analog-to-digital converter should be placed as near as possible to the antenna in the chain of front end components and the resulting samples should be processed using a programmable microprocessor. The potential problems of analog components, like non-linearization, temperature shifting and so on, will not happen to digital processors. And the programmability enables a single front-end with the flexibility

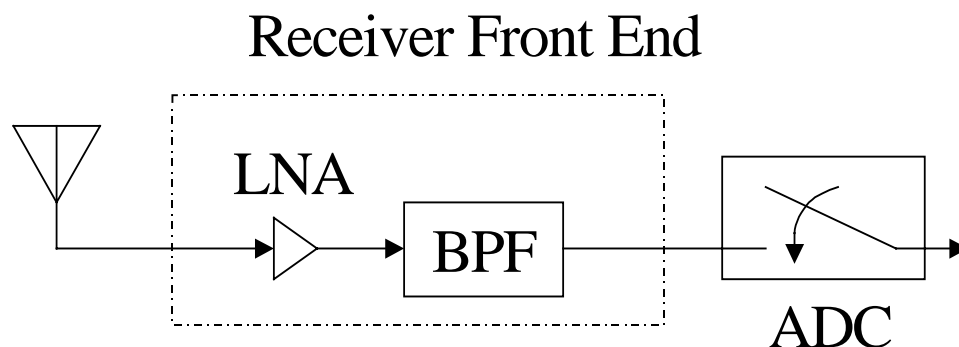


Fig. 3. 14 Structure of Software Radio Receiver Digitized Front-end [Akos, 1997]

of dealing with various incoming signals, with different carrier and bandwidth with efficient CMOS/VLSI implementation [Mitola, 1995].

For a GPS C/A code receiver, the processor is designed with FFT blocks to calculate correlation functions. Computation capability and speed need to be concerned and efficient FFT algorithm should be designed.

3.6 Hardware Implementations

Hardware design of software GPS receiver has been proposed [Gunawardena, 2000] with 5000 point FFT and iFFT (inversed FFT) blocks. Considering the processing complexity and speed requirements, field programmable gate array (FPGA) is available for this implementation. Performance degradations caused by the finite precision of hardware computations were also simulated. The effects of truncation and quantization were analyzed. As the conclusion, acquisition in FPGA is still realistic and can be efficiently performed within limited programmable hardware.

However, it has been further found that acquisition with 5000 point FFT is not easy to be accomplished in real time even with the powerful FPGA devices. Alternative algorithms are needed to make the FFT computation feasible.

4 AVERAGING

Sampling frequency needs to be no less than twice the signal bandwidth determined in front end according to Nyquist's law. For example, when bandwidth is set to be 2MHz in a receiver, sampling rate can be 5 Msps. Receivers also have to up sample local C/A code up to this rate in order to compute correlation functions. Since the period of C/A code is 1 millisecond (ms), the samples from this 1 ms will be put together to do block processing. There are 5000 samples per ms. Thus the correlation of 5000 samples needs to be performed. As discussed in Section 3.6, 5000 points FFT is too expensive to implement in hardware, which might be the reason why the frequency domain processor is not popular in present GPS receivers. However, there have been FFT blocks for 1024 points designed by Xilinx. The original C/A code chip rate is 1023 per millisecond. If the received signal can be recovered back to the same rate as C/A code, the computation can thus be implemented in the 1024 FFT blocks. This chapter shows how to use the 1024 FFT blocks to do the software signal processing in frequency domain, which is the basic idea for hardware implementation of C/A code acquisition.

4.1 Averaging Up Sampled Signal

In order to compute correlation functions in 1024 point FFT block, the method called "Averaging Correlation" [Tsui, 2000] [Starzyk, 2001] is introduced here.

The received signal needs to be reduced back to 1023 chips per millisecond by averaging consecutive 4 or 5 points into one chip. The averaged chip is similar to a chip of C/A code. Since the signal cannot be observed in forms of square waves, there is not enough information to determine which 4 or 5 points should be grouped together and averaged. Unless there can be an approach to know the relative position of the samples and the chips. Although this relative position cannot be exactly found, a rough estimates can be found out from several attempts of averaging with different assumption of the relative position, as displayed in Fig. 4.1

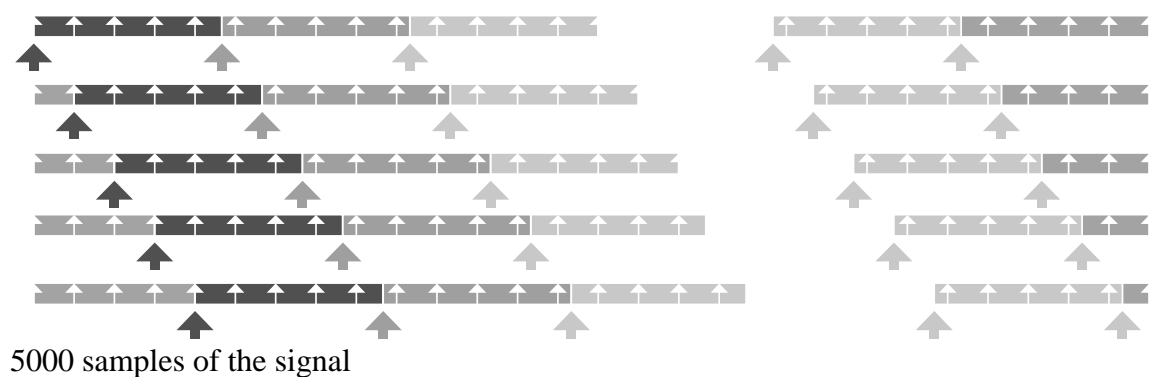


Fig. 4. 1 The 5 Sequences of Averaged Steps

Among the first consecutive 5 samples, one of them must be the first sample of a chip, since no chip contains more than 5 samples. Assuming this sample is regarded as the beginning position of the first chip, the relative position of the 1023 chips and all the samples can be determined and the chips can be recovered completely. Although that beginning point would not be the exact starting position in normal cases and in reality it

may start at the middle of two samples (in the worst case, as in Fig. 4.2) this recovered sequence is a fairly good approximation of original chips, only suffering the loss of energy around 10%. However, the sequence that has the largest correlation peak does not necessarily have the largest noise sample, acquisition margin can be retained. Peak-to-peak ratio measurement shows the averaging even behaves slightly better than direct correlation without averaging, as shown in succeeding sections.

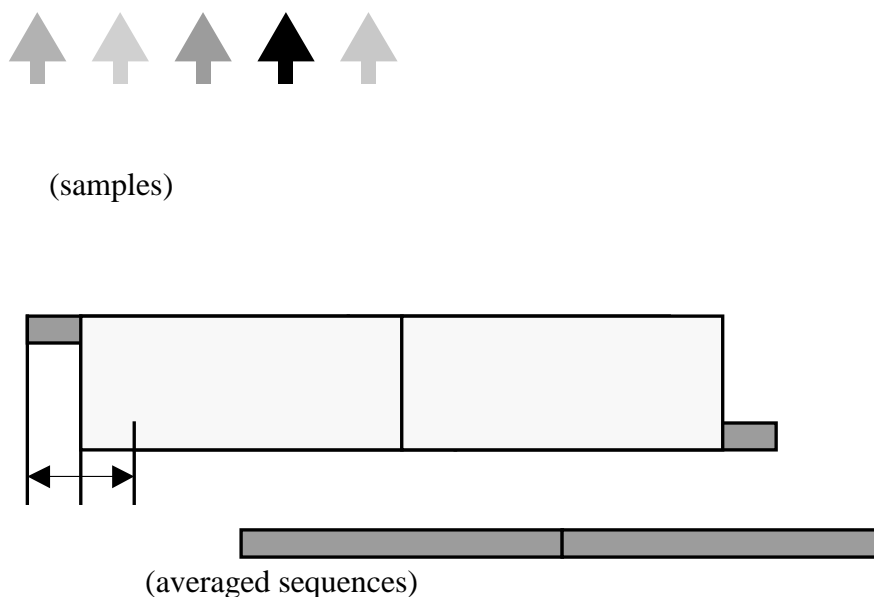


Fig. 4. 2 Worst Case of Code Phase

Thus the problem is reduced to searching for the beginning sample of the first chip within the 5 averaged sequences, as shown in Fig.4.1. Thus 5 averaged sequences, each containing 1023 chips, are generated and their correlation functions with local C/A code are computed respectively. Knowing the correlation peak indicates the signal

energy, the sequence with the largest correlation peak is chosen as the one used for acquisition.

However, all the five correlation functions can be observed as sampling the continuous correlation function at different places, or different relative shift of the received signal and the local code. They can be interleaved to form a whole correlation function, which consists of $5 \cdot 1023$ samples. Actually the time location of each one of these values represents a particular relative shift in time domain between the received signal and the local code. Obviously the shift represented by the largest peak is nearest to the code phase. The way to precisely locate the code phase will be discussed in section 4.4, which is denoted to signal tracking.

4.2 Acquisition with Smaller FFT Blocks

With the 5 averaged sequences and 1023 chips C/A code, the correlation must be performed 5 times. Notice that 5 times 1023 FFT is still much cheaper than 5000 FFT performed once, no matter in hardware or just software simulation in MATLAB. In addition, if the averaging correlation is used in signal tracking where the peak location is roughly known, only 3 averaged sequences near the peak need be used thus further reducing the computation effort.

In the case this method is only applied to rough acquisition, when the received signal is strong enough the correlation of one or two out of these 5 sequences with C/A code can already locate the peak at chip level, as shown in Fig. 4.4 and Fig. 4.5.

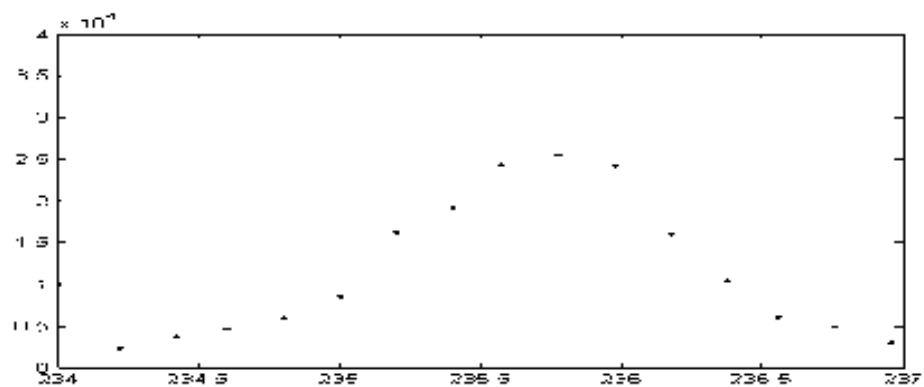


Fig. 4. 3 Discrete Correlation (part)

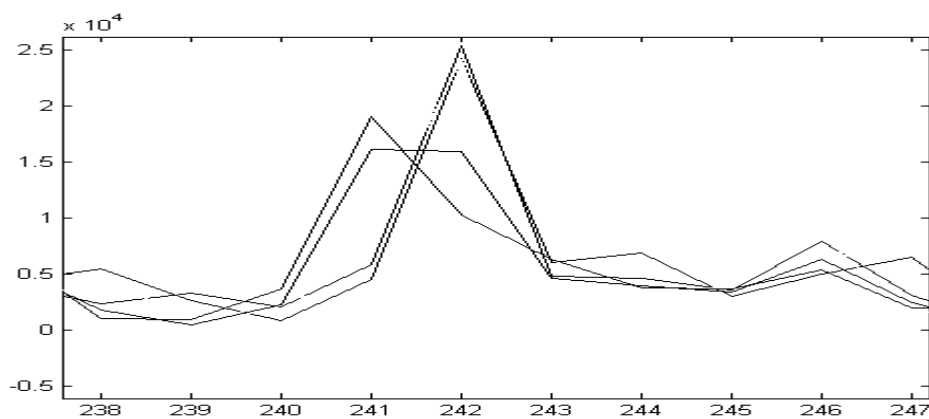


Fig. 4. 4 Correlation Result for Each of the 5 Sequences and C/A Code [Starzyk, 2001]

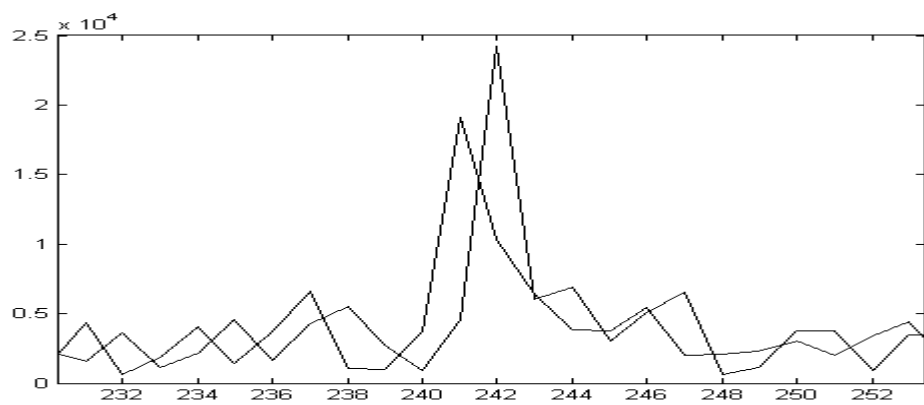


Fig. 4. 5 Correlation Result for 2 of the 5 Sequences and C/A Code [Starzyk, 2001]

A good point of “averaging correlation” is that it is not going to reduce the peak-to-peak ratio (in another word, acquisition margin) compared with correlation by 5000 FFT. As discussed in section 3.3.2, this ratio is related to misdetection probability and must not be compromised.

When the correlation result of the C/A code with one out of the 5 sequence has the largest peak value among all 5 sequences’ correlation functions, this sequence is considered to be the best recovery of the original chips within the received signal, as discussed in Section 3.1. The peak-to-peak ratio is computed based on the correlation of this sequence and is compared with the peak-to-peak ratio obtained from 5000 FFT correlation function. The performance related misdetection probability of averaging correlation can be estimated in this way. This comparison was carried out based on 200 consecutive milliseconds of received GPS signal. Statistical results shown in Fig.6 and 7 indicate that the performance of the averaging method won’t be worse than 5000 FFT correlation, if not better.

In Fig. 4.6, the dashed line stands for peak-to-peak ratio obtained from the correlation function by 5000 point FFT over 200 millisecond data. The mean ratio is 2.3675 with the variance 0.0915, as illustrated in Fig. 4.7. The continuous line stands for the similar ratio from the correlation function obtained by averaging method also over 200 milliseconds. Its mean value is 2.5776 with variance 0.1144, as in Fig. 4.8. From mean values it can be

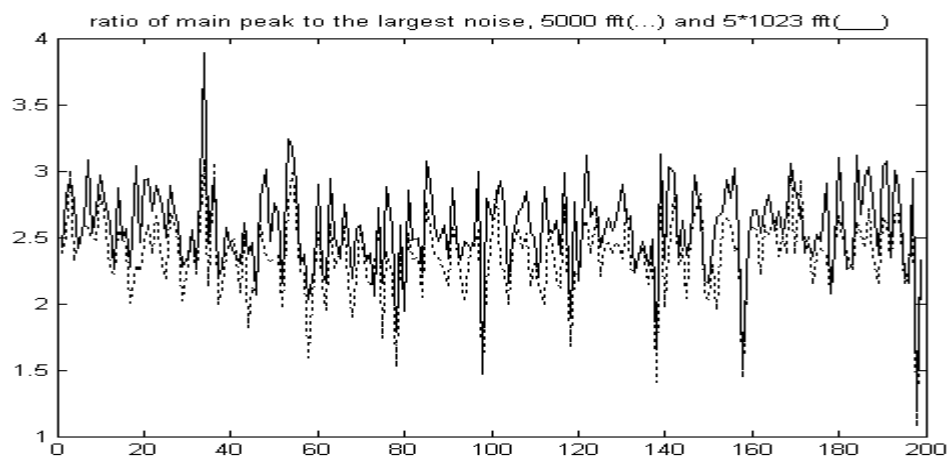


Fig. 4. 6 Peak-to-peak Ratio Comparison of the Two Methods
(Over 200 Millisecond Data) [Starzyk, 2001]

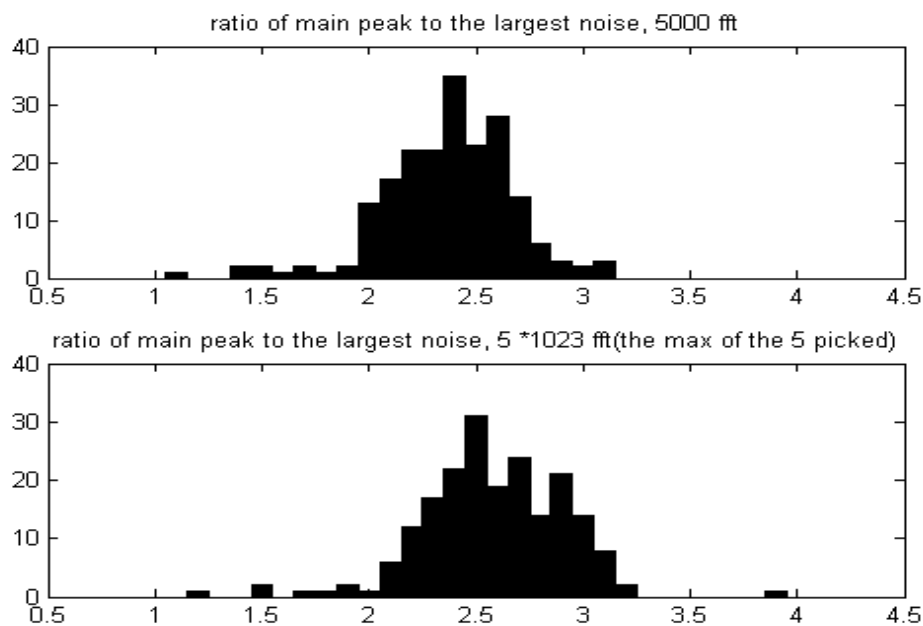


Fig. 4. 7, 4. 8 Peak to the Second largest Ratio, Comparison of Two Methods
[Starzyk, 2001]

found that averaging method seems a little bit more stable than the 5000 FFT correlation, in terms of acquisition margin. Fig. 4.7 and 4.8 indicate the histogram of this two ratio values through out the 200 milliseconds of data.

In the conclusion, the averaging correlation can work as well as the original correlation method based on 5000 Msps with no averaging in signal acquisition and is less expensive to implement.

4.3 Correlation using Block Processing

As mentioned above, the biggest advantage of the averaging correlation computation is that it can be implemented in 1024 point FFT block processing, which is proven to be convenient and efficient. However, the length of averaged sequences in this method is designed the same as a pure C/A code to be 1023 chips, which makes it unable to be directly implemented in block processing.

4.3.1 Zero Padding

A normal approach to do 1023 point FFT in a 1024 point FFT block is to do zero padding, as applied in some of the computation and simulation software, such as Matlab. If the zero padding method is realized by adding one more chips of zeros at the end of the sequence, it may cause a big problem when applied in circular correlation.

Assuming received signal S has been averaged to a shifted C/A code sequence with noise

$$\text{Seq}[n] = A([\text{CA}[k+1:1023], \text{CA}[1:k]]) + \text{Noise}$$

After zero padding, C/A and Seq are changed into:

$$\text{CA0} = [\text{CA}, 0]$$

$$\text{Seq0} = [\text{Seq}, 0],$$

as Fig. 4.9 shows for $k = 511$.

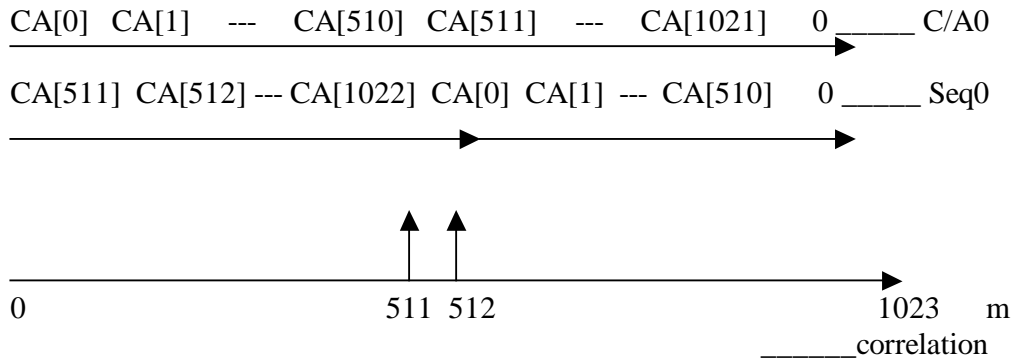


Fig. 4. 9 Correlation Zero Padding Sequences

Using circular correlation definition of eq3.17

$$\Phi_{\text{Seq0CA0}}[m] = \text{Seq0}[n] \otimes \text{CA0}[n] = \sum_{n=0}^L \text{Seq0}[n] \text{CA0}[\text{mod}(n-m, L+1)] \quad (4.1)$$

Where m indicates relative shift between Seq and CA, $L = 1023$.

There will be two correlation peaks appearing at shift of k and $k+1$, as shown in

Fig. 4.9. The peak at k is expressed as:

$$\Phi_{\text{Seq0CA0}}[k] = \sum_{n=k}^{L-1} \text{Seq}[n] \text{CA}[\text{mod}(n-k, L+1)] + 0 \times \text{CA}[L-k] + \sum_{n=0}^{k-2} \text{Seq}[n] \text{CA}[\text{mod}(L-k+n+1, L+1)] + 0 \times \text{Seq}[k-1]$$

In the case Seq is shifted C/A code with noise:

$$\begin{aligned}
\Phi_{Seq0CA0}[k] &= A \sum_{n=k}^{L-1} CA[\text{mod}(n-k, L+1)]CA[\text{mod}(n-k, L+1)] + \\
&\sum_{n=k}^{L-1} noise[n]CA[\text{mod}(n-k, L+1)] + 0 \times CA[L-k] + \\
&A \sum_{n=0}^{k-2} CA[\text{mod}(L-k+n, L+1)]CA[\text{mod}(L-k+n+1, L+1)] + \\
&\sum_{n=0}^{k-2} noise[n]CA[\text{mod}(L-k+n+1, L+1)] + 0 \times Seq[k-1]
\end{aligned} \tag{4.2}$$

Notice that the first component of the summation represents the correlation energy of the corresponding parts from Seq and CA while the other components are either noise or not matching.

Therefore this correlation function could be represented by two parts as in Eq. 4.3:

$$\Phi_{Seq0CA0}[k] = A(L-k) + N1 \tag{4.3}$$

Where $A(L-k)$ is the signal energy and $N1$ stands for all the other components produced in Eq. 4.2.

Using the same logic as above, peak at $k+1$ is:

$$\begin{aligned}
\Phi_{Seq0CA0}[k+1] &= \sum_{n=k+1}^{L-1} Seq[n]CA[\text{mod}(n-k, L+1)] + 0 \times CA[L-k-1] + \\
&\sum_{n=0}^{k-1} Seq[n]CA[\text{mod}(L-k+n, L+1)] + 0 \times Seq[k]
\end{aligned} \tag{4.4}$$

$$\Phi_{Seq0CA0}[k+1] = Ak + N2 \tag{4.5}$$

Also $N2$ stands for all the other items here.

It can be seen that each of these two peaks can be expressed in two terms, desired correlation signal energy and correlation noise. Correlation energy in these two peaks can

be combined and form the energy of the correlation peak equal kL . The noise terms consist of correlated noise and undesired partially correlated signal energy in N_1 and N_2 respectively. They may become main noise source in tracking, as discussed in the next sections. However, their effects are negligible in acquisition since normally acquisition does not have strict requirements of precision.

The two peaks separate the whole energy into two parts, A_k and $A(L-k)$. Apparently it breaks the structure of the “circular correlation”. In the worst case, the code phase k can be nearly half of the whole code length $L = 1023$ as in Fig 4.9, $k = 511$. As a result, the added “zero” chip will break this received C/A code into two parts with roughly the same length. These two parts can be correlated with the local code separately and form two nearby correlation peaks $\Phi_{Seq0CA0}[k]$ and $\Phi_{Seq0CA0}[k+1]$, with nearly the same strength. Therefore the largest loss of energy can be up to 50%, that is 3 dB. Loss of this signal energy and correlation peak results in larger probability of misdetection discussed in section 3.4.

On the other hand, there can be an extremely ideal case. When the Seq has the same phase as the CA, that is, $k = 1023$, zero chips are padded at the end of both of them, as shown in Fig 4.10:

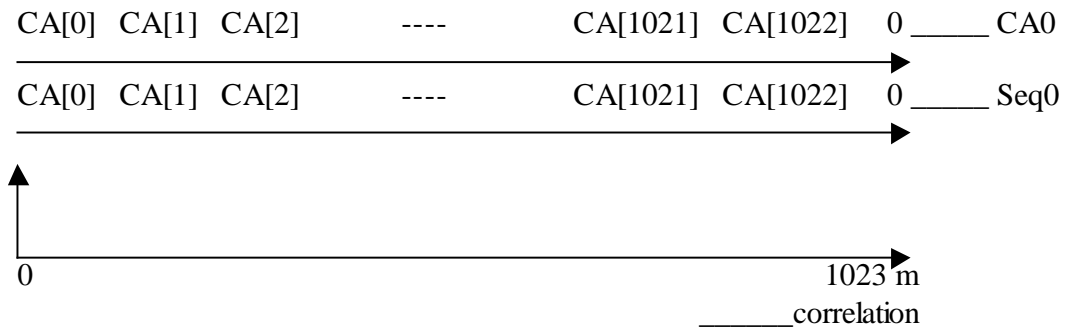


Fig. 4. 10 Correlation of Zero Padding Sequences, $k = 1023$

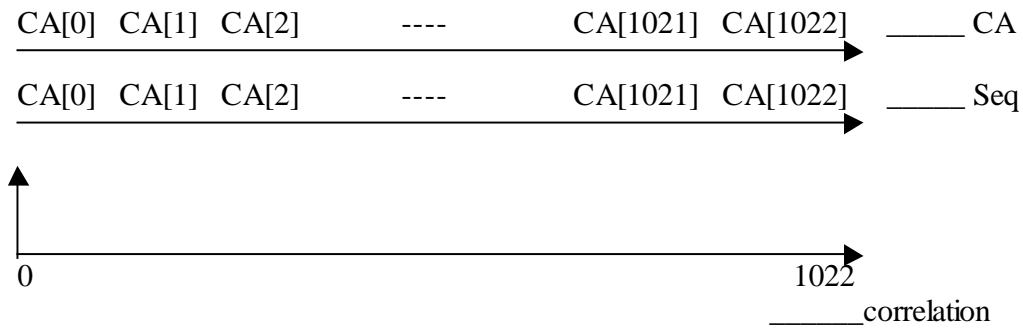


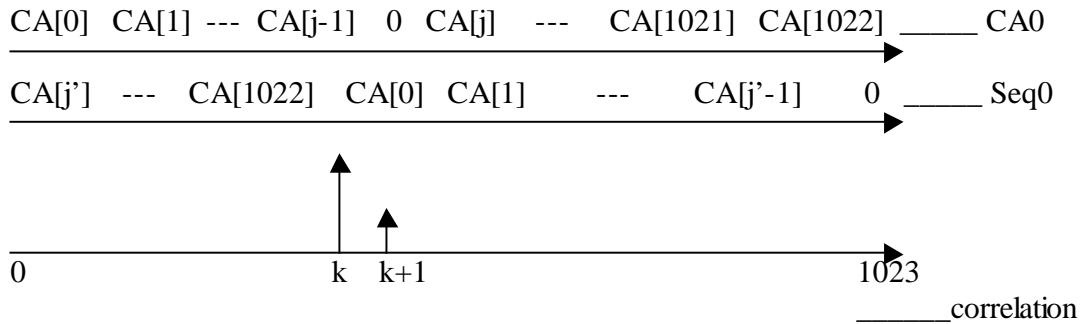
Fig. 4. 11 Correlation of Non-zero Padding Sequences

The peak $\Phi_{Seq0CA0}[k]$ obtained from correlation by zero padding FFT completely represents the correlation energy as obtained through 1023 point FFT correlation, as in Fig. 4.11. There appears to be no energy loss in this case. It can be extended to a general case, whenever the zero chip is padded at code phase k in CA, there won't be energy loss.

Based on this fact, it is reasonable to attempt several different places j 's of zero padding in CA instead of simply putting a zero after all the other chips, in order to have $k' = L-j+1$ close enough to the unknown code phase k . So that the two separated peaks

cannot share the whole signal correlation energy evenly, as $\Phi_{Seq0CA0}[k] \gg$

$\Phi_{Seq0CA0}[k+1]$ or $\Phi_{Seq0CA0}[k] \ll \Phi_{Seq0CA0}[k+1]$, as shown in Fig. 4.12.



Where $j' = L - k + 1$.

Fig. 4. 12 Correlation of Zero Padding Sequences, at Selected Places

Let:

$$CA0 = [CA[0:j-1], 0, CA[j:L-1]];$$

$$Seq0 = [Seq 0];$$

As in Eq.4.1

$$\Phi_{Seq0CA0}[m] = Seq0[n] \otimes CA0[n] = \sum_{n=0}^L Seq0[n] CA0[\text{mod}(n - m, L + 1)]$$

When $k' < k$,

$$\begin{aligned} \Phi_{Seq0CA0}[k] &= \sum_{n=k}^{L-1} Seq[n] CA[\text{mod}(n - k, L + 1)] + 0 \times CA[L - k] + \\ &\sum_{n=0}^{k-k'} Seq[n] CA[\text{mod}(L + n - k + 1, L + 1)] + 0 \times Seq[k - k' + 1] \\ &\sum_{n=k-k'+2}^{k-1} Seq[n] CA[\text{mod}(L + n - k + 2, L + 1)] \end{aligned} \quad (4.6)$$

Ignoring all the noise and undesired terms

$$\Phi_{Seq0CA0}[k] = A(L - k + k') \quad (4.7)$$

When $k' > k$, it is straight forward to find that

$$\Phi_{Seq0CA0}[k] = A(k' - k) \quad (4.8)$$

There are two divided correlation signal energy parts with the loss of $\frac{k' - k}{L}$ and $\frac{L - (k' - k)}{L}$ respectively. Since the larger one out of these two peaks will be picked as the “acquired” correlation peak, the largest loss is no more than 50%, as argued above.

However, j can be tried with different values:

$$j_i = \text{floor}\left(\frac{i}{H}L\right), i \leq H, j_i \in J_s \quad (4.9)$$

Where J_s is a set of H integer values indicating the location of the inserted 0.

So that there can be $2H$ peaks obtained. The largest one out of these $2H$ peaks would only suffer the loss no more than $\frac{1}{2H}$ of correlation energy with no noise enhancement.

H has been set as 2, 3 and 4 respectively to examine the loss of signal energy, in term of peak-to-peak ratio. As discussed in the previous chapter, peak-to-peak ratio is used as a representative of misdetection probability to measure to acquisition performance. Experiments show that averaged peak-to-peak ratios of $J = 2, 3$ and 4 are lower than the ratio obtained using direct averaging correlation. Where direct averaging

correlation here indicates the correlation that is computed without any zero padding or other skills to fit in the size of FFT block 1024.

Previous analysis has already shown that direct averaging correlation can provide higher peak-to-peak ratio compared with 5000 point correlation. And the ratios from zero padding method ($J = 3$ or 4) still appear higher than that obtained through 5000 point correlation, which indicates that zero padding averaging correlation has achieved better acquisition performance.

4.3.2 Modified C/A Code [Alaqeeli, 2001]

The zero padding method introduced in the previous section brings in another search of the padding place. Although the signal energy loss is limited to $\frac{1}{2H}$, as discussed in section 4.3.1, averaging correlation computation also needs to be repeated for J times, according to Eq. 4.9, which makes the cost of either time or hardware resource (FFT blocks) J times larger. Having critical hardware implementation limitations, zero padding may not be a good solution for frequency domain correlation realization.

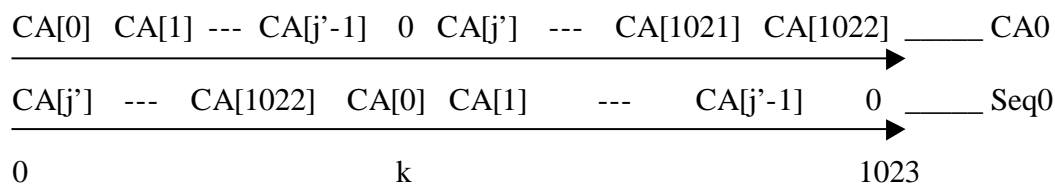
Another solution of computing averaging correlation using 1024 point FFT block has been worked out, named as Modified C/A Code [Alaqeeli, 2001], which is to rescale both the received sequence and the local C/A code into 1024 samples and fit into the FFT block size.

The received signal is originally continuous waveform and has been digitized with the sampling rate of 5000 Msps. It can be down sampled into 1023 points to do correlation with C/A code. However, the down sampling rate can be arbitrarily selected so that signal can also be down sampled into 1024 points per millisecond. It should be noticed that same processing must be done on local C/A code. This way Modified C/A Code is generated. The two modified code sequences, instead of original C/A code sequences, are fed into 1024 point FFT blocks directly, since they both have 1024 samples. The correlation can be completed efficiently. Experiments show that roughly there is 13% loss in averaged peak-to-peak ratio compared with 5000 point correlation.

4.4 Correlation Based Tracking

By calculating the discrete correlation functions, correlation based tracking can be accomplished. As discussed, triangular shape fitting will be used onto the discrete correlation function.

Based on the acquisition results, rough code phase can be obtained on the chip level. Correlation function can be done based on this rough code phase. The local C/A code CA is expanded into a 1024 points sequence CA0 by padding a zero at k , which is assumed to be in the same place for the received signal, as shown in Fig. 4.13:



Where $j' = L - k + 1$.

Fig. 4. 13 Correlation of Zero Padding Sequences, Based on Acquisition

As discussed before, 5 averaged sequences are generated which in practice are not lined up with local C/A code. For these sequences, zero padding will not cause any extra error to the averaging correlation. The correlation functions obtained from these 5 sequences are interleaved and form a whole correlation with 5115 points.

As mentioned in section 4.1, the 5 correlation functions obtained using these averaged sequences can be observed as sampling the continuous correlation function at different places. Each point from these correlation functions is corresponding to a unique relative shift value of the received signal and the local code, as mentioned in section 3.4.2. Since correlation is a function of the relative shift, all these 5115 points can be collected to form a new discrete correlation function, as shown in Fig. 4.14.

Triangular fitting method is applied for code phase tracking, as shown in Fig. 3.13. This method is based on the fact that the peak of C/A code auto correlation is shaped as an isosceles triangle and its width is 2 chips [Braasch, 1999]. The height of this triangle is determined by signal energy, as mentioned in section 3.1. Since signal energy is difficult to precisely detect directly from the correlation function, normally the height of this triangle is unknown. Therefore a triangle with the width of 2 chips and a

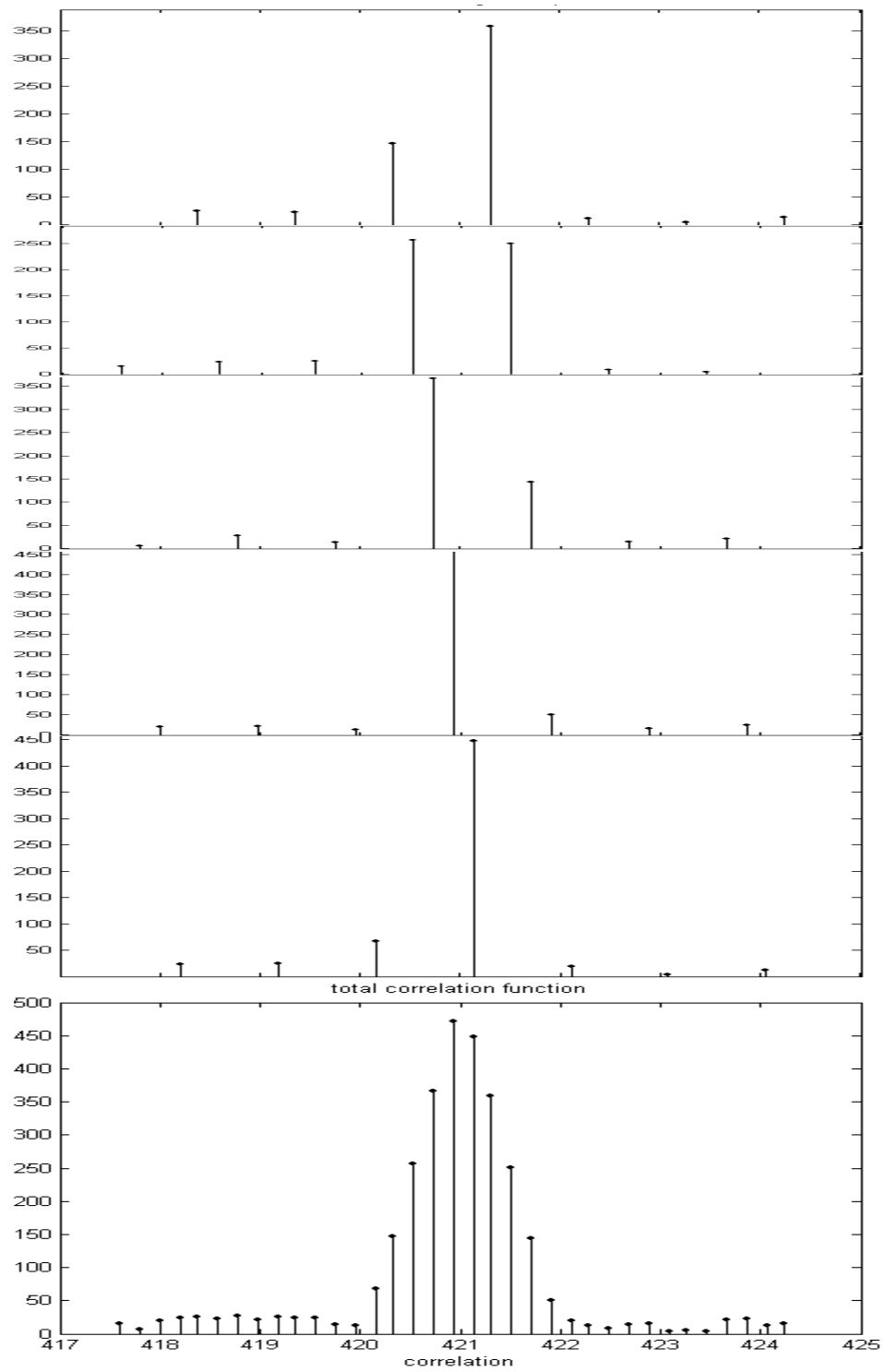


Fig. 4. 14 Forming A Discrete Correlation

flexible height can be used to approximate the peak of the correlation function. This triangle should be fit closest to the points that represent the peak in the discrete correlation function.

The largest 3 points in the correlation function are used to determine the unknown parameters of that fit-in triangle, location of the top x_0 (in code phase domain) and height y_0 , as shown in Fig.4.15. x_0 is regarded as the result of tracking, the code phase of the signal. However, the highest point in the correlation function is much more noisy than the other two points (shown as (x_1, y_1) and (x_2, y_2) in Fig. 4.15), due to signal distortion and other error sources. In practice only these two points are used to locate the fit-in triangle.

Let d_1 and d_2 be the distances from these two points to the triangle. To minimize d_1 and d_2 , x_0 can be determined:

$$x_0 = (y_2 \cdot x_1 - y_1 \cdot w + y_1 \cdot x_2) / (y_1 + y_2) + w / 2 \quad (4.10)$$

Where $w = 2chips \cong 1.955\mu s$. Thus $d_1 = d_2 = 0$.

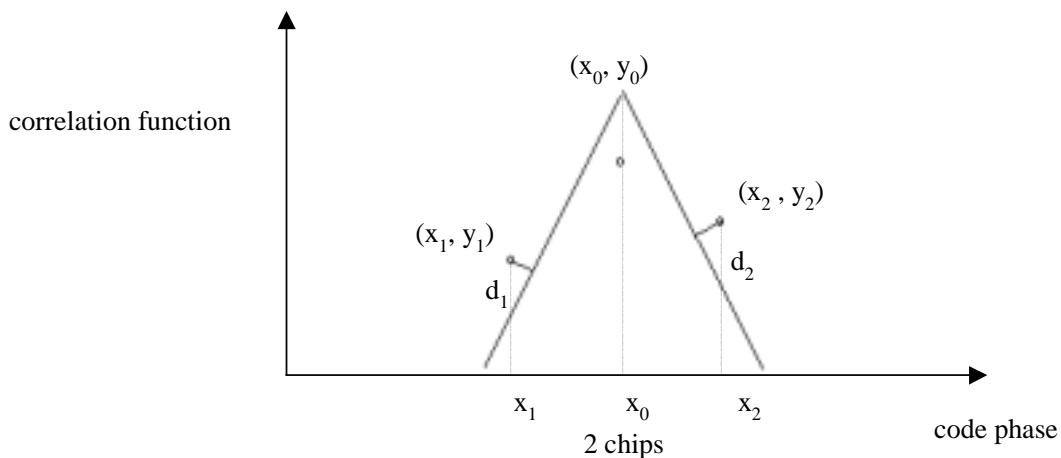


Fig. 4. 15 Fit-in Triangle

Accumulated tracking error is a function of accumulation window size, as shown in Fig. 4.16. Assuming the incoming signal has the same code phase for at least 5 seconds, the window can be as large as 5 seconds. As can be observed at the end of the curve in Fig. 4.16, the averaged code phase has the error around 3.3 ns, which is equivalent to an error of 1 meter in pseudo range measurement.

It should be noted that signal averaging is equivalent to a low pass filter. This effective filter does not have linear phase characteristics so that additional tracking error may be introduced in this way.

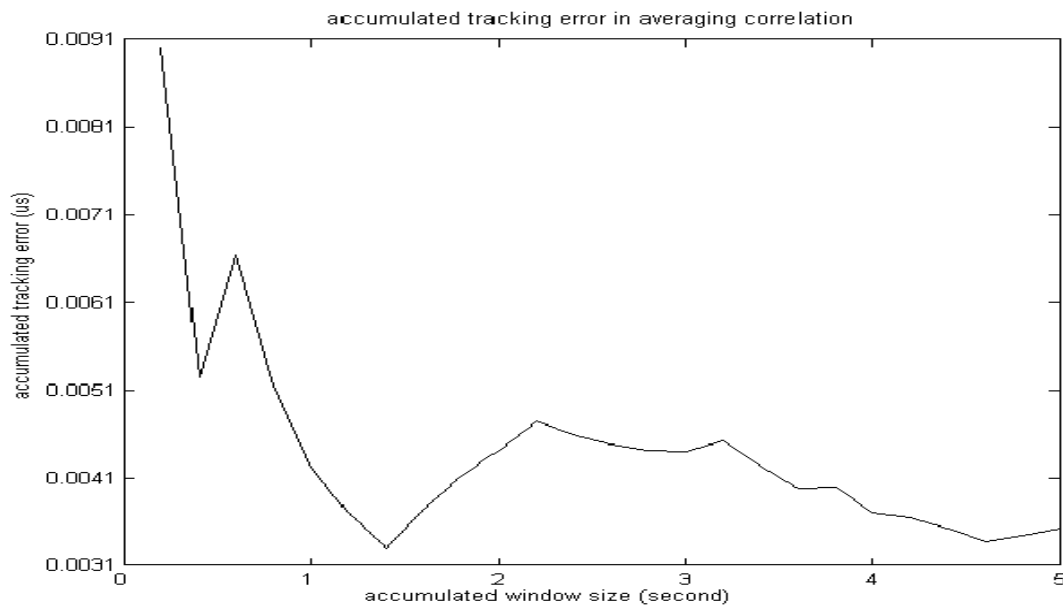


Fig. 4. 16 Accumulated Tracking Error

5 WEAK SIGNAL ACQUISITION

In the previous chapter all the concerned signal processing was based on a single period of the C/A code, which is 1 millisecond long. Although this single period can be used for tracking and pseudo range measurement can be obtained from it, there may not be enough energy in it. For instance, a single millisecond signal suffers great acquisition misdetection probability when carrier to noise ratio drops below 43 dB-Hz, as described in Chapter 3.

Unfortunately, high carrier to noise ratio is not likely to happen at the same time for the signals received from all the satellites. Only few satellites with high elevation angle can be observed with C/N_0 large enough to have tolerable misdetection probability, for example, $C/N_0 > 43$ dB-Hz. Other satellites, which have lower elevation angle, have their signals suffer from more shadowing, more atmospheric loss and less antenna pattern gain. They cannot be acquired by just using 1 ms C/A code signal. For individual mobile users, they can hardly receive any GPS signal's direct component when they are indoors, a problem similar to weak mobile phone signals. Weak signal acquisition is especially concerned for the indoor mobile GPS users. Therefore new GPS receivers designed for those users must be capable of processing very weak signal. Existing commercial receivers are able to acquire signals with C/N_0 of 35-37 dB-Hz [Psiaki, 2001]. Receivers may be able to acquire weaker signals if navigation data bit transitions can be previously located.

Generally, the way to acquire weak signal is to accumulate energy from consecutive time slots [Lin, 2000]. Some accumulation methods can run beyond the data

bit transition boundaries, by taking the magnitudes. The price is smaller carrier to noise ratio gain and larger interference residues. Another accumulation may need more precise demodulating frequency. Thorough search of IF requires much larger computation capability to handle. Block addition technique will be applied and compared with other energy accumulation methods. It is proven to be efficiently limiting interference.

5.1 Accumulation

Signal energy needs to be accumulated over a period of time because it is too weak to do direct acquisition. Here is an example of accumulation:

$$\begin{aligned}
 R[m] &= \sum_{j=0}^{N-1} (s[k + jL] + n[k + jL]) * CA[k] \\
 &= \left(\sum_{j=0}^{N-1} s[k + jL] \right) * CA[k] + \left(\sum_{l=0}^{N-1} n[k + jL] \right) * CA[k] \quad (5.1)
 \end{aligned}$$

Where $s[k]$ is the digitized received signal, noise free. “*” stands for correlation computation, either sequential or circular. Particularly, $s[k]$ repeats C/A code each millisecond and the code length is L . Thermal noise $n[k]$ is assumed to be an Additive White Gaussian Random Process with standard deviation σ .

Equation 5.1 only provides a basic model of accumulation in the carrier free case. Demodulation effects need to be considered in practice.

5.1.1 Gain on Carrier to Noise Ratio

In the case $s[k+jL] = s[k]$, the accumulated signal is

$$s_{Nacc}[k] = \sum_{j=0}^{N-1} s[k + jL] = Ns[k]. \quad (5.2)$$

As a result the signal power has been increased N^2 times:

$$P_{Nacc} = N^2 P_s$$

The correlation function of the signal and C/A code becomes N times larger:

$$\sum_{j=0}^{N-1} s[k + jL] \otimes CA[k] = N \cdot s[k] \otimes CA[k] \quad (5.3)$$

At the same time noise items are also summed up:

$$n_{Nacc}[k] = \sum_{l=0}^{N-1} n[k + jL] \quad (5.4)$$

Unlike C/A code, noise item $n[k]$ is assumed to be time uncorrelated:

$$E(n(k)n(k+1)) = 0 \quad (1 \neq 0)$$

Accumulated noise item n_{Nacc} therefore has the variance [Papoulis, 1965]:

$$\text{var}(n_{Nacc}) = N\text{var}(n)$$

As a result the noise power is enhanced N times. Thus the equivalent carrier to noise ratio of this accumulated signal becomes N times larger than that of single millisecond of received signal, or $10\text{Log}N$, in dB. As discussed in section 3.3, larger C/N_0 improves the acquisition performance with smaller misdetection probability. It can be clearly observed from Fig. 3.7 that the misdetection probability decreases dramatically as C/N_0 becomes larger. For example, a weak GPS signal may have its C/N_0 as weak as

35 dB-Hz, which corresponds to a misdetection probability of near 100%, in another word, very unlikely to be acquired. However, when N is set to be 10, accumulation improves C/N_0 by 10 dB. Misdetection probability becomes low enough with $CNR = 45\text{dB}$ and acquisition is feasible.

Based on the assumption of random noise, accumulation method can be used in weak GPS signal, especially, C/A code acquisition.

5.1.2 Effect on Signal Bandwidth and Interference

Despite the improvement of misdetection probability, accumulation also narrows down the signal bandwidth. The accumulating window size N millisecond results in the

signal bandwidth of $\frac{1}{N\text{ms}} = \frac{1}{N}\text{kHz}$.

For instance, in normal acquisition $N=1$, which corresponds to the signal bandwidth of $\frac{1}{1\text{ms}} = 1\text{kHz}$. When $N=10$, it shrinks into $\frac{1}{10}\text{kHz}$. This narrow bandwidth is actually beneficial to the weak signal acquisition by filtering in-band interferences, although it also requires thorough frequency search.

The incoming signal contains components from all the “visible” satellites instead of only from the one being acquired. In acquisition the correlation function of all the components of the signal with the desired local C/A code is computed, this function consists of two parts. One is the correlation of the component from the acquired satellite and local code, which represents the signal energy. The other part contains the cross correlations due to other satellites.

C/A code has bounded cross correlation, as one of its basic features, as shown in Chapter 3. Cross correlation of C/A code is considered as the main source of in-band interference. Although all the satellites' signals are modulated at the same L1 frequency, they still have difference in carrier frequency when received, due to different Doppler effects. Because of this difference, the self-interference caused by cross correlation is located at the carrier frequency slightly different from the desire signal. With the same received signal power, cross correlations are limited to be same level of auto correlation side lobe, which is 12 dB weaker than auto correlation peak. In that sense, self-interference won't cause significant increase in misdetection probability. But the assumption of equal signal power for all satellites cannot be applied to the weak signal acquisition case [Capozza, 2000].

For example, signal from low elevation angle satellites can be more than 20dB weaker than that from high elevation angle satellites. Unfortunately, when the receivers need to acquire the low angle satellites, the interference signal is much stronger than the acquired one. The self-interference can be around the same or even above the level of the correlation peak of the acquired C/A code. Obviously interference brings in higher misdetection probability compared with the interference free case at the same noise level.

As mentioned in chapter 3, both the auto correlation and cross correlations behave as a function of demodulation frequency deviation and time window size N . Because all "visible" satellites always have different motion relative to the user, they have different Doppler effects on carrier and produce inter-frequency interference. At the output of the receiver front end, those IF values are also deviated variously. After the signal has been

demodulated with a proper frequency, which is the same or close to IF carrying the desired signal, all the other cross correlations have the problem of demodulation frequency deviation. Their magnitudes decline as functions of IF deviation and N , which will be discussed in section 5.5.3.

Therefore, self-interference can be depressed due to the frequency deviation, and larger N provides better performance in limiting interference as well as accumulating greater signal energy, according to Eq. 3.13.

However, the correlation function also becomes more sensitive to the frequency deviation when N grows larger. In order to avoid energy loss, frequency search needs to be carried out more carefully. More search steps will be implemented, as shown in section 5.5.1. Resource cost and consumed time are the price of larger N .

It should also be noted that navigation data is spread on the top of the C/A code. Twenty C/A code periods are used to express a single data bit. Bit transitions should also be taken into account in choosing N . Because of this limitation, N has to be less than 20, which may not be good enough in extremely weak signal cases, as for indoor receivers. There is another option to accumulation. Receivers can sum the energy from K discontinuous pieces of signal, where each piece is N millisecond long.

The accumulation procedure has been realized in different ways.

5.2 Time Domain Process

In modern civil receivers, time domain processing is used. For instance, non-coherent demodulation and sequential correlators may use these equations [Psiaki, 2001]:

$$\begin{aligned}
 R^2[m] = & \sum_{j=0}^{K-1} \left(\left[\sum_{n=jNL}^{(j+1)NL-1} s_j[n] \cdot CA[\text{mod}(n-m, L)] \cdot \cos[\Omega_j n] \right]^2 \right. \\
 & \left. + \left[\sum_{n=jNL}^{(j+1)NL-1} s_j[n] \cdot CA[\text{mod}(n-m, L)] \cdot \sin[\Omega_j n] \right]^2 \right), 0 \leq m < L
 \end{aligned} \tag{5.5}$$

Or:

$$\begin{aligned}
 |R[m]| = & \sum_{j=0}^{K-1} \left\{ \left| \sum_{n=jNL}^{(j+1)NL-1} (s_j[n] \cdot \cos[\Omega_j n] + i \cdot \sum_{n=jNL}^{(j+1)NL-1} (s_j[n] \cdot \sin[\Omega_j n]) \right. \right. \\
 & \left. \left. \cdot CA[\text{mod}(n-m, L)] \right) \right\}, 0 \leq m < L
 \end{aligned} \tag{5.6}$$

Where $s[n]$ is the received signal with noise, CA is the locally generated C/A code, Ω is the IF and $R[m]$ is the complex correlation function. Each N millisecond block is taken out of the received signal as a whole piece. As can be seen from the above equations, each piece is incoherently demodulated and correlated with C/A code. The energy of this piece is accumulated as the peak of correlation function. After that, those pieces are combined as R^2 and $|R|$. For each piece, signal power becomes N^2 times larger and noise variance increases N times at the same time:

$$P_{Nacc} = N^2 P_s$$

$$\text{var}(n_{Nacc}) = N \text{var}(n)$$

When $N = 1$ and $K = 1$, Eq. 5.5 and Eq. 5.6 are exactly the same for normal acquisition. N cannot be larger than 20 due to the navigation data, which means that the accumulating window cannot be larger than 20 ms. Usually N is set as 10 [Psiaki, 2001].

Obviously each one out of K pieces of signal is demodulated using a unique IF respectively. Since in acquisition the phase of IF carrier normally is unknown, non-coherent demodulation is used for all the pieces. Because these K pieces are taken independently, they do not have any deterministic relationships in their phases, which means that they have to be demodulated separately. Their in-phase and quadratural components could not be directly added up as for the N milliseconds of data. Instead, the magnitudes of the K pieces of complex signal are summed up.

It should be noted that the K pieces of signal have been accumulated. Obviously signal power is increased K^2 times in this case:

$$P_{Kacc} = K^2 P_{Nacc}$$

Similarly, noise variance is also enhanced K times due to the accumulation. However, noise distribution is changed by taking the magnitudes, which results in larger misdetection probability. Experiments show that the effect of taking magnitudes of noise is approximately equivalent to double the noise variance in this case. Therefore noise variance has been increased $2K$ times:

$$\text{var}(n_{Kacc}) = 2K \text{var}(n_{Nacc})$$

It should also be noted that K is not sensitive to the data bit transition because the magnitudes instead of the original signals are used in accumulation in Eq. 5.5 [Psiaki, 2001]. Unlike the accumulation method of window size N discussed in section 5.1.1, K

can be larger than 20. Beyond this limitation, more signal energy could be exploited in weak signal acquisition. However, larger value of K won't be able to narrow down the bandwidth, because each one out of the K pieces of the signal is demodulated independently in this method.

Another assumption, which was previously made for Eq. 5.5 and 5.6, is that the IF is regarded as unchanged during each accumulating time window N . Since both the satellites and receivers may be moving fast and their Doppler effects are changing, IF could not stay constant despite its deviation from the designed value. This assumption needs to tolerate signal energy loss in addition to that caused by demodulating frequency search imprecision. It should also be noticed that the IF search step would be no larger than $\frac{1}{2N}$ kHz as discussed in section 5.2, for maintaining enough signal energy.

In conclusion, carrier power is increased $(KN)^2$ times while noise variance is enhanced $2KN$ times:

$$P_{Kacc} = (NK)^2 P_s$$

$$\text{var}(n_{Kacc}) = 2NK \text{var}(n)$$

Therefore the improvement in Eq. 5.5 and Eq. 5.6 on C/N_0 is $KN/2$.

Based on the two equations and the frequency search step size, the time domain weak signal acquisition can be realized in 2-D search, similar to the normal acquisition. Correlation of N milliseconds of signal as a whole block is actually equivalent to overlapping a block of signal onto a single period, or 1 millisecond. In order to

implement correlation more efficiently, frequency domain process is used with FFT blocks, as argued in Chapter 4.

5.3 Frequency Domain Process

A similar principle of accumulation can be applied to frequency domain processing. An accumulation method in frequency domain processing has been proposed [Psiaki, 2001],

$$|R[m]| = \sum_{j=0}^{K-1} \left| \left\{ iFFT \left[FFT \left(\sum_{l_j=0}^{N-1} s_{l_j}[n] \cdot \cos[\Omega_j n] + i \cdot \sum_{l_j=0}^{N-1} s_{l_j}[n] \cdot \sin[\Omega_j n] \right) \cdot FFT^*(CA[n]) \right] \right\} \right| \quad (5.7)$$

Although Eq. 5.7 aims to compute correlation function of received signal and local C/A code, it has been carried out in a way different than what is described in Eq. 5.6. Obviously frequency domain circular correlation replaces of time domain correlation of Eq. 5.7. Similar as discussed in the previous section, C/N_0 is improved $K/2$ times. In the case the accumulation is after the correlation calculation, this method can be called Post Correlation Overlapping.

Advantage of taking $N = 1$ with large K is that data bits would not cancel the energy accumulation since the magnitudes instead of complex correlation functions are summed up. Therefore this accumulation can go on as long as the receiver hardware can support. The following analysis shows the computation when K is 10. For mobile users, acquisition time should be limited to no more than several minutes. Although frequency domain process can speed up the acquisition, large amount of computation is still

unaffordable. Therefore it is reasonable to set $K = 10$ as the accumulation time window size.

The block size N is set to be 1, which means that a block is only a single millisecond of signal in this case. As discussed in Chapter 3, GPS receivers normally cannot afford large FFT blocks in hardware implementation. The applicable FFT block size is only suitable for processing 1 ms data and could be realized with averaging correlation efficiently. However, self-interference could not be depressed in this case since signal bandwidth is not changed, as will be demonstrated in section 5.5.3. Therefore this method loses the ability of resisting self-interference in addition to less C/N_0 improvement. It needs to be modified for weak signal acquisition problem. Block size N makes it difficult for FFT blocks to process on, but the whole data block can be overlapped and added to fit the FFT blocks. Thus Block addition technique is proposed.

5.4 Block Addition for Weak Signal Acquisition

It should be noticed that

$$\begin{aligned}
 R'[m] &= \sum_{j=0}^{K-1} iFFT(FFT(s_j[n]) \cdot FFT(CA[n])^*) \\
 &= iFFT(FFT \sum_{j=0}^{N-1} (s_j[n]) \cdot FFT(CA[n])^*)
 \end{aligned} \tag{5.8}$$

Where $N = K$.

This equation shows two forms of a frequency domain correlation function in IF free case. Note that the first form actually follows Eq 5.7, Post Correlation Overlapping.

Although there seems no difference between the two forms since $N = K$, the N millisecond signal is continuous in the second form, while in the first form K millisecond signal is not in general. As in time domain processing, they can be demodulated compactly as in Eq. 5.6. While in the first form, K blocks of signal are demodulated separately before they are added together. The two forms are really different in sense of bandwidth and IF search step, as discussed at the beginning of this chapter.

On contrary, in the second form of Eq. 5.8, the whole N millisecond signal is shifted together and overlapped onto 1 millisecond time window before correlation. The actual bandwidth is $1/N$ kHz instead of 1 kHz, since the shifting and overlapping in time domain just mean phase changing and summation in frequency domain, according to the Fourier Transform Theory.

$$f(t - T) \leftrightarrow F(\omega)e^{j2\pi T} \quad (5.9)$$

As the result, IF search step becomes $\frac{1}{2N}$ kHz instead of 0.5 kHz for the first form. At the same time, the self-interference from cross correlation will also be limited. This overlapping can be realized as “Block Addition” [Gunawardena, 2000], as follows.

$$|R[m]| = \left| \{ iFFT[FFT(\sum_{j=0}^{N-1} s_j[n] \cdot \cos[\Omega n] + i \cdot \sum_{j=0}^{N-1} s_j[n] \cdot \sin[\Omega n]) \cdot FFT^*(CA[n])]\} \right| \quad (5.10)$$

5.5 Performance Comparison

The three accumulation methods, time domain process, Post Correlation Overlapping and Block Addition correlation were analyzed using a block of 10 ms

continuous GPS C/A signal to simulate weak signal acquisition. The signal is generated with pre determined noise level and an arbitrary code phase. Their performance of resultant carrier to noise ratio and computation costs will be examined and compared.

For time domain process, $N = 10$ and $K = 1$:

$$|R_1[m]| = \left| \sum_{n=0}^{10L-1} (s[n] \cdot \cos[\Omega n] + i \cdot (s[n] \cdot \sin[\Omega n]) \cdot CA[\text{mod}(n-m)]) \right|, \quad (5.11)$$

$$0 \leq m < L$$

At each frequency search step of the 2-D search process, signal is demodulated and correlated with expanded C/A code. Correlation function is obtained in time domain processing.

Note that at each step IF is regarded as constant during the 10 ms, according to the assumption made in section 5.2. So the signal bandwidth is $\frac{1000Hz}{NK} = 100Hz$

Frequency search step could be 50Hz in this case, as suggested in section 5.2. In this case we also assume that Doppler Frequency is located within the range of +/- 5KHz as normal for GPS signal.

For Post Correlation Overlapping method, $N = 1$ and $K = 10$. The signal bandwidth is thus 1 KHz and the IF search step for each millisecond data can be as large as 0.5 KHz.

$$|R_2[m]| = \sum_{j=0}^9 \left| \{ iFFT[FFT(s_j[n] \cdot \cos[\Omega_j n] + i \cdot s_j[n] \cdot \sin[\Omega_j n]) \cdot FFT^*(CA[n])] \} \right| \quad (5.12)$$

For Block Addition Correlation, $N = 10, K = 1$.

$$\begin{aligned}
|R_3[m]| = & \left| \{ iFFT [FFT ((\sum_{j=0}^9 s_j[n]) \cdot \cos[\Omega n] \right. \\
& \left. + i \cdot (\sum_{j=0}^9 s_j[n]) \cdot \sin[\Omega n]) \cdot FFT^* (CA[n]) \} \right| \quad (5.13)
\end{aligned}$$

The signal bandwidth is thus $1/N = 100\text{Hz}$ and the IF search step for each millisecond data can be as large as 50Hz , which are the same as for time domain process.

5.5.1 Carrier to Noise Ratio Gain

Compared with no accumulation, the three methods result in different gain values in carrier to noise ratio into acquisition. Those gain values result in less misdetection probability, as can be seen in section 3.3.2. Based on simulated signal of $C/N_0 = 30\text{ dB-Hz}$ and 35 dB-Hz respectively, the comparison experiment is repeated for 200 times. The mean peak-to-peak ratios over those experiments are listed in Table 5.1 as to directly observe the effects. However, this comparison is based on the assumption that no bit transition occurs in the 10 ms signal block. Otherwise bit transitions may cause signal energy cancellation when Block Addition is used. Since one navigation data bit occupies 20 ms , Block Addition needs to be applied to two continuous blocks simultaneously so that at least one of these two blocks does not have a bit transition inside. It should be noted that the accumulation window size for Post Correlation Overlapping could go far beyond 10 ms . As a result, larger C/N_0 gain can be achieved using Post Correlation Overlapping. The three correlation functions have different acquisition margins. Simulation results based on signal with $C/N_0 = 38\text{ dB}$ are provided as examples in Fig. 5.1, 5.2 and 5.3 respectively.

Table 5. 1 C/N₀ Gain Comparison of Correlation Methods (on 10 ms signal)

	R1	R2	R3
Gain	10 dB	7dB	10dB
Averaged Peak-peak ratio (35 dB-Hz)	2.17	1.74	2.17
Misdetection Probability (30 dB-Hz)	11%	45%	11%
BW	100 Hz	1kHz	100 Hz

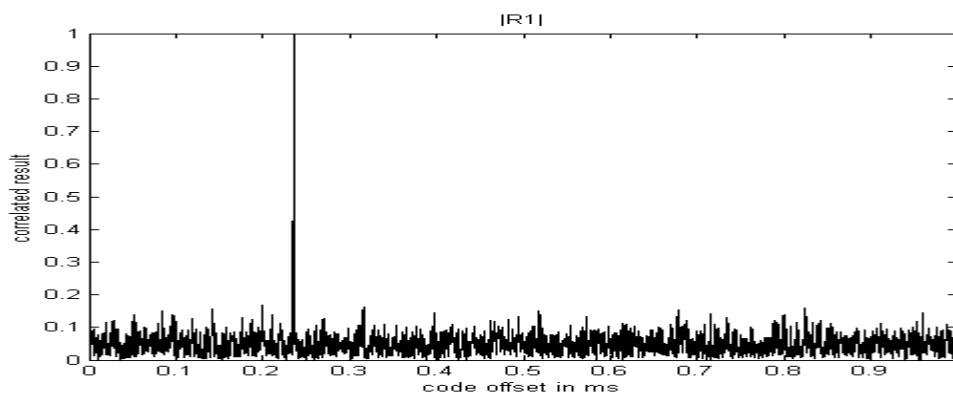


Fig. 5. 1 Correlation Using Sequential Accumulation Process

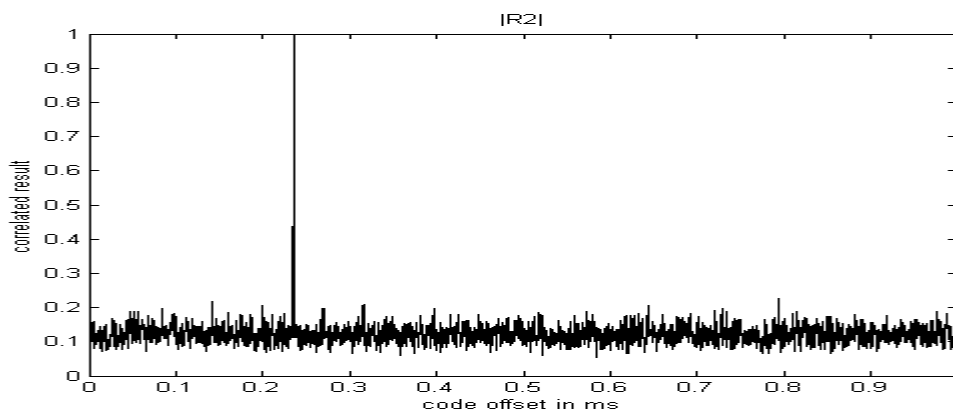


Fig. 5. 2 Correlation Using Post Correlation Overlapping

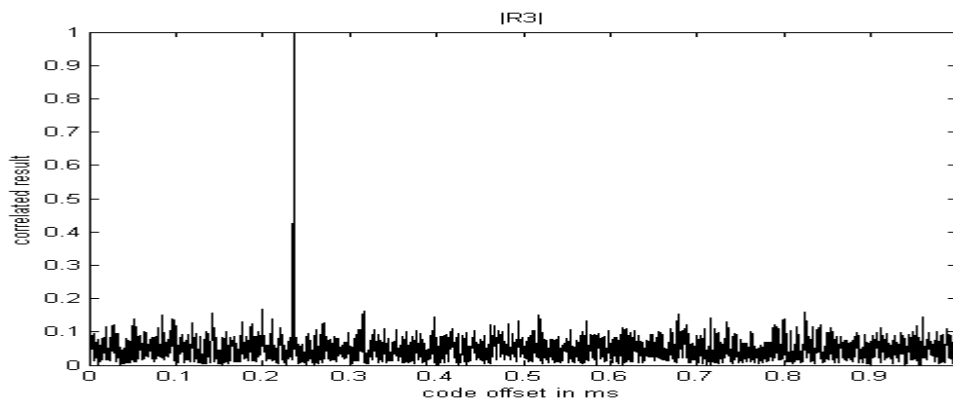


Fig. 5. 3 Correlation Using Block Addition Correlation

Correlations using $|R1|$, $|R2|$ and $|R3|$ all provide large acquisition margin in this weak signal situation. As can be seen from Fig. 5.1, 5.2 and 5.3, $|R1|$ and $|R3|$ seem to be equivalent. Remember that $|R2|$ is taking summation of the magnitude of the correlation function obtained from each millisecond signal and C/A code. Apparently the noise level in Fig. 5.2 is higher compared with $|R1|$ and $|R3|$. The performance of $|R1|$ and $|R3|$ is desired in weak signal acquisition and further information will show that the acquisition with $|R3|$ is easier to achieve.

5.5.2 Computation Cost and Time

Based on the IF search steps and range size (± 5 kHz assumed) the computation cost as well as the approximate time for acquisition can be estimated. According to the previous discussion, $|R1|$ is extremely time consuming. As for 2-D search, the sequential correlation will be processed at each step. Using the IF range of 10 kHz, IF search step of 50 Hz and code phase search of 1023 chips, the time consumption could be estimated as: $10\text{ms} \times 1023 \times 10\text{k}/50 = 2046\text{s}$. In order to avoid the cancellation caused by data bit transition, acquisition using $|R1|$ has to be carried out on two continuous accumulation windows. The receiving time needs to be doubled to 4092s in this case. In reality, receivers can save part of the signals in their internal memory so that the receiving time can be shortened to less than 1 minute. Otherwise the receiving time is unacceptable to mobile receivers.

With the same conditions of IF, $|R2|$, $|R3|$ can complete the code phase search using circular correlation. The correlation function is obtained based on a single piece of

signal. Therefore expected signal receiving time is only 10ms. However large amount of FFT computation cost is demanded for both of them. Using |R2| to compute correlation in 2-D search, there are 20 IF search steps and at each step 30 times FFT/iFFT processes are necessary. Similarly, there are 200 IF steps using |R3| and at each step 3 times FFT/iFFT are needed. Together they need 600 times FFT/iFFT computations. Using the averaging correlation method introduced in Chapter 4, each 5000 point FFT/iFFT needs to be implemented with 5 times 1024 point FFT/iFFT. Using Virtex FPGA technology, a 1024 point FFT/iFFT can be accomplished in 4145 clock cycles. Having a clock of 40 MHz, a 1024 point FFT/iFFT roughly costs 0.1 ms. Therefore acquisition using |R2| and |R3| is expected to be finished in 0.3 seconds. Considering data bit transitions, time consumption becomes twice as larger, that is, 0.6 second.

Method |R2| and |R3| is much more efficient than time domain processing. Although method |R3|, Block Addition Correlation consumes more time than method |R2|, Post Correlation Overlapping Correlation, both of them are acceptable for weak signal acquisition. However, not only does Block Addition provide larger C/N_0 gain, but also it suppresses self-interference, as mentioned in section 5.1.

5.5.3 Interference Depression

Comparing the three methods, it should also be noted that the signal bandwidth should be taken into account. Although no interferences can be observed from these plots, they would happen in really weak signal cases.

Table 5. 2 Computation Cost Comparison of Correlation Methods (on 10 ms signal)

	R1	R2	R3
BW	100 Hz	1kHz	100 Hz
Gain	10 dB	7dB	10dB
IF step	50 Hz	500Hz	50Hz
IF range	10 kHz	10 kHz	10 kHz
Computation cost per IF step (FFT times)	-	30	3
Total Cost (FFT times)	-	600	1200
Receiving time	4092s	10ms	20ms
Acquisition time	-	0.3s	0.6s

Interfered signal is simulated as follows:

Acquired signal is assumed perfectly demodulated, while the interference source has different Doppler frequency and there is some IF residual components in it after demodulation. As for weak signal acquisition case, desired signal is decided to be 20 dB below a single self-interference signal.

For |R1| and |R3|, this interference, in another word, (normalized) cross correlation function is the function of N and IF residue:

$$S(\omega, B_s) = \left(\frac{\sin(0.5\Delta\omega / B_s)}{0.5\Delta\omega / B_s} \right)^2$$

Where $B_s = \frac{1}{N} kHz$, $N = 10$. For example, when IF residue is 450 Hz, $\Delta\omega = 900\pi \text{ rad/s}$, $S = -23\text{dB}$. Thus the interference becomes 23 dB weak after accumulation.

For |R2|, it is not related to N:

$$S(\omega, B_s) = \left(\frac{\sin(0.5\Delta\omega / B_s)}{0.5\Delta\omega / B_s} \right)^2, B_s = 1kHz$$

Also assuming IF residue is 450 Hz, $S = -3\text{dB}$. Interference depression is only 3 dB, which is the same as for no accumulation normal correlation.

Fig 5.4 and 5.5 show that method |R3| provides larger acquisition margin than |R2|, when there is strong self-interference.

Block Addition Correlation is much more powerful in weak signal acquisition in large interference background.

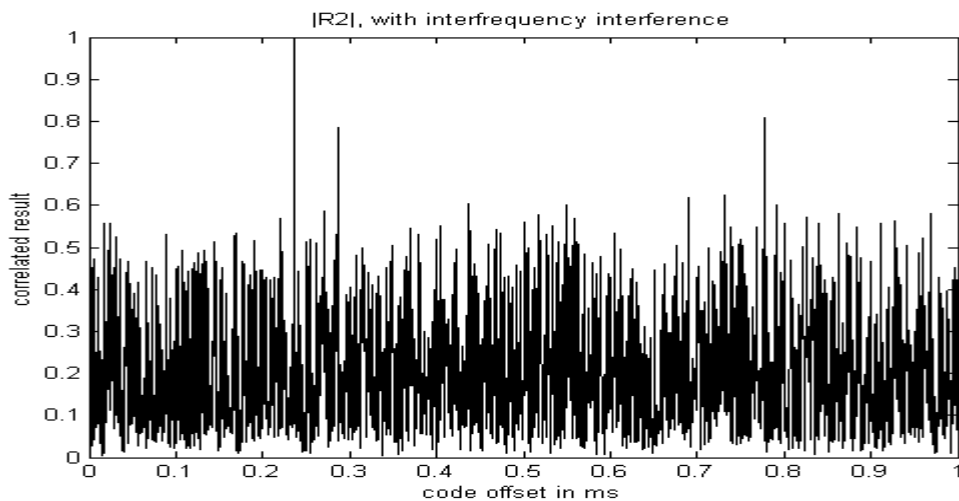


Fig. 5. 4 Post Correlation Overlapping, with Interference

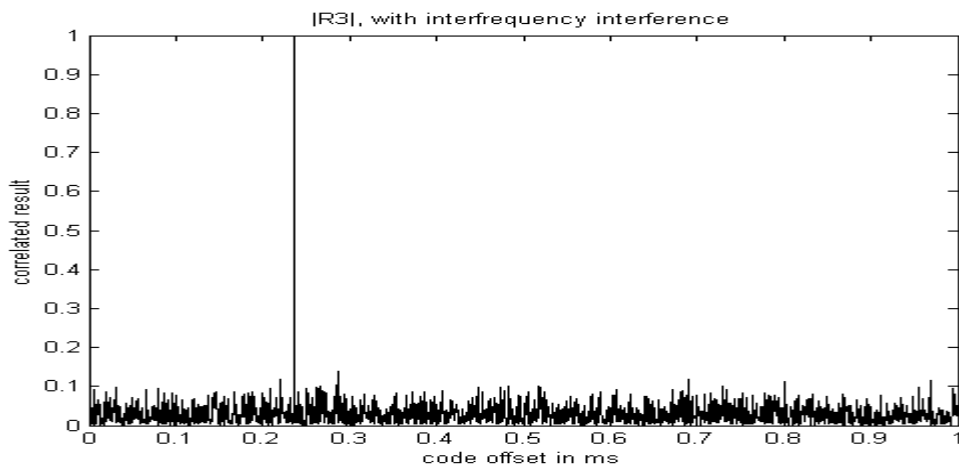


Fig. 5. 5 Block Addition Correlation, with Interference

5.6 Discussions of Block Addition

5.6.1 Accumulation Window Size and Navigation Data Bit

In previous discussions it has been always mentioned that 10 millisecond is selected as accumulation window size considering navigation data bit transition. Navigation data is transmitted at 50 bps, which indicates a possible bit transition each 20 millisecond. Window size larger than 20 milliseconds may have the cancellation problem in block addition. In reality two independent acquisition procedures will be performed based on continuous two sets of 10 milliseconds of signal. One of them must have been executed within the same bit range and will be chosen as the Block Addition Correlation result.

If accumulation window of 20 milliseconds has to be used, bit transition position will be searched. Larger computation cost becomes unavoidable. It will be more reasonable to combine this search with navigation data demodulation.

5.6.2 Combination of Block Addition and post correlation overlapping

It can be found that the frequency domain processing corresponding to time domain Eq. 5.6 is:

$$\begin{aligned}
 |R[m]| = & \sum_{k=0}^{K-1} \left| \{ iFFT[FFT((\sum_{j=0}^{N-1} s_j[n]) \cdot \cos[\Omega n] \right. \\
 & \left. + i \cdot (\sum_{j=0}^{N-1} s_j[n]) \cdot \sin[\Omega n]) \cdot FFT^*(CA[n]) \} \right| \quad (5.14)
 \end{aligned}$$

This is actually a combination of the two frequency domain accumulation methods. Although it needs more FFT calculations, it could go over data bit transition and achieve better acquisition capability in weaker signal cases. For instance, $N = 10$ and $K = 10$, C/N_0 gain can be 17 dB-Hz, which means that in the worst case, acquirable signal's C/N_0 is 26 dB-Hz and signal bandwidth is 100 Hz. Computation cost increases by 10 times in this case so that more powerful FFT block is expected.

5.6.3 Efficient Realization with Averaging

It has been proven that small sized FFT process blocks can be applied to solve 5000 FFT problems using Averaging Correlation, as proposed in chapter 4. Block Addition correlation can be implemented more efficiently using averaging techniques. Fig. 5.6 shows the correlation based on simulated signal of $C/N_0 = 38$ dB-Hz, which is the same as the base of Fig. 5.1 through 5.3. Using a weak signal with $C/N_0 = 35$ dB-Hz, averaged peak-to-peak ratio is 2.35, which is slightly worse than the ratio of 2.17 obtained using direct Block Addition as shown in table 5.1. Signal bandwidth is not changed using averaging method.

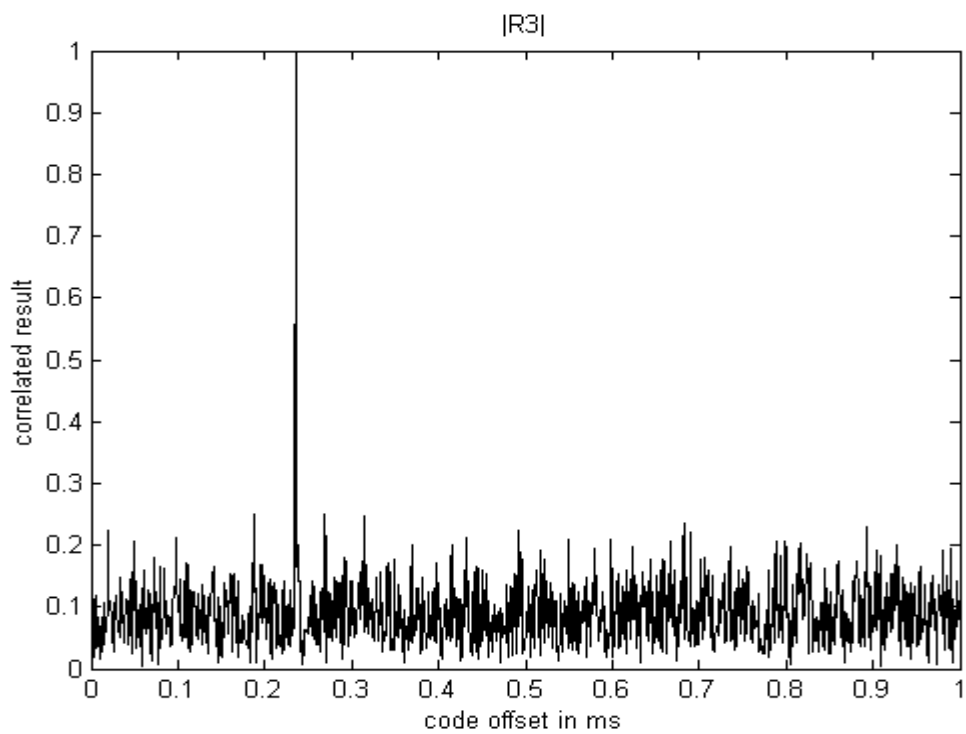


Fig. 5. 6 Block Addition Averaging Correlation

6. CONCLUSION AND FUTURE WORK

This research has been devoted to GPS SPS signal acquisition and tracking algorithm design. Frequency domain processing has been proposed as an efficient solution of correlation computation. A new method named “Averaging Correlation” is introduced as a realizable implementation of correlation. Weak signal acquisition methods are analyzed and evaluated. The method Block Addition has been found powerful and convenient. All the algorithms aim to provide mobile GPS users better positioning services with fewer limitations.

Correlation function is the fundamental of GPS signal acquisition and tracking. With the help of software radio technology correlation can be calculated in frequency domain using FFT. “Averaging Correlation” has been designed to implement the circular correlation in small general FFT blocks. Frequency domain processing of GPS signal becomes more realistic using this method. Tracking techniques based on correlation function are also introduced, which is also different from traditional tracking methods. Averaging Correlation provides the basic functional block for weak signal processes.

For mobile GPS users, weak signal acquisition has been a major difficulty. Accumulation of signal energy has been proposed to increase carrier to noise ratio. Three major developed accumulation methods are compared with their performance and availability. It has been demonstrated that Block Addition method, which can be realized using averaging correlation, can efficiently accumulate signal energy with limited noise enhancement. At the same time it was found in this work that Block Addition depresses

self-interference by limiting incoming signal bandwidth. Therefore Block Addition is proven to be a good solution for weak GPS signal acquisition.

Major effort in this thesis has been on software simulation. Hardware implementation of a frequency domain mobile GPS receiver design will be goal of future works. The succeeding stage of acquisition and tracking is the navigation data demodulation, which can also be realized using the Block Addition technique has been invested but has not been included in this thesis.

REFERENCE

- [1] Akos, Dennis M. (1997), "A Software Radio Approach to Global Navigation Satellite System Receiver Design", Ph. D. Dissertation, Ohio University, August
- [2] Akos, D.M., Normark, P. L., Enge, P., Hansson, A. and Rosenlind, A. (2001), "Real-Time GPS Software Radio Receiver", *National Technical Meeting Proceedings*, January
- [3] Alaqeeli, Abdulqadir (2001), Personal Communications, Athens, Ohio, December
- [4] Bose, V. G. (1999), "The Impact of Software Radio on Wireless Networking," *Mobile Computing and Communications Review*, Volume 3, No. 1, January
- [5] Braasch, Michael S. and van Dierendonck A. J. (1999), "GPS Receiver Architectures and Measurements", *Proceedings of The IEEE*, VOL. 87, No. 1, January
- [6] Capozza, Paul T., Holland, Brian J. Hopkinson, Thomas M. and Landrau, Roberto L. (2000), "A Single-Chip Narrow-Band Frequency-Domain Excisor for a Global Positioning System (GPS) Receiver", *IEEE Journal of Solid-State Circuits*, VOL. 35, NO. 3, March
- [7] Feng, Gang and van Graas, Frank (1999), "GPS Receiver Block Processing", ION GPS, Nashville, Tennessee, September

- [8] Hegarty, Christopher J. (1999) "Evaluation of the Proposed Signal Structure for the New Civil GPS Signal At 1176.45 MHz", work note, MITRE CORP, June.
- [9] Gold, R. (1967), "Optimal Binary Sequences for Spread Spectrum Multiplexing", *IEEE Trans. Inform. Theory*, VOL. IT-13, pp. 619-621, October
- [10] Gunawardena, Sanjeev (2000), "Feasibility Study for the Implementation of Global Positioning System Block Processing Techniques in Field Programmable Gate Arrays", Master Thesis, Ohio University, November
- [11] Kaplan, Elliott D. Editor (1996), Understanding GPS-Principles and Applications, Artech House Publishers, ISBN: 0890067937
- [12] Kayton, Myron and Fried, Walter R. (1997), Avionics Navigation Systems, 2nd Edition. John Wiley & Sons, INC. ISBN: 0471547956.
- [13] Lin, David M. and Tsui, James B.Y. (2000), "Comparison of Acquisition Methods for Software GPS Receiver", ION GPS, Salt Lake City, Utah, September
- [14] Mitola, Joe (1995), "The Software Radio Architecture", *IEEE Communications Magazine*, VOL. 33, No. 5, pp. 26-38, May

- [15] Papoulis, Athanasios (1965), Probability, Random Variables, and Stochastic Processes, McGraw-Hill, Inc.
- [16] Psiaki, Mark L. (2001), “Block Acquisition of Weak GPS Signals in a Software Receiver”, ION GPS, Salt Lake City, Utah, September
- [17] Starzyk, J. and Zhu, Zhen (2001) “Averaging Correlation for C/A Code Acquisition and Tracking in Frequency Domain”, MWSCS, Fairborn, Ohio, August
- [18] Stuber, Gordon L. (2001), Principles of Mobile Communication, 2nd edition, Kluwer Academic Publishers, ISBN: 0792379985
- [19] Tsui, James B. Y. (2000), Fundamentals of Global Positioning System Receivers: A Software Approach, Wiley, John and Sons, Incorporated, ISBN: 0471381543
- [20] Uijt de Haag, Maarten (1999), “An Investigation Into the Application of Block Processing Techniques for the Global Positioning System”, Ph. D. Dissertation, Ohio University, August

ABSTRACT

Zhu, Zhen, M. S. March, 2002

Electrical Engineering

Averaging Correlation for Weak Global Positioning System Signal Processing (81 pp.)

Director of Thesis: Dr. Janusz A. Starzyk

Weak signal processing capability is desired for those GPS receivers designed for individual mobile users. However it requires large amount of computation, which is not affordable to traditional GPS receivers. Using software technology and Block Processing techniques, signal can be processed in frequency domain, which improves GPS receivers' processing power. Therefore the GPS receivers implemented with software technology can be applied in the weak signal situation.

Basic stages of GPS signal processing include signal acquisition and tracking, which are both based on the correlation functions. In order to efficiently compute the correlation functions for GPS C/A code in hardware, a method named "Averaging Correlation" is proposed in this thesis. Using this method, receivers can implement correlation computation in small general-purpose processing blocks and require less hardware effort. Therefore frequency domain acquisition can be conveniently realized in GPS receivers, which is different from the time domain sequential processing in traditional receivers. The tracking technique based Averaging correlation is also discussed.

However, acquisition for weak GPS signal requires accumulation of signal energy. Several algorithms for weak GPS signal acquisition have been proposed. These algorithms are analyzed and evaluated in this thesis. Their performance and hardware cost are compared. One of them, Block Addition is found with better performance, especially with the existence of large interference. It is also suggested that Block Addition can be applied in navigation data demodulation. Block Addition can be realized using Averaging Correlation.

Approved: _____

Signature of Director